A bending-active gridshell as falsework and integrated reinforcement for a ribbed concrete shell with textile shuttering: Design, engineering, and construction of KnitNervi

Lotte Scheder-Bieschin [a,*], Serban Bodea [a], Mariana Popescu [b], Tom Van Mele [a], Philippe Block [a]

[a] Institute of Technology in Architecture, Block Research Group, ETH Zurich, Stefano-Franscini-Platz 1, 8093 Zurich, Switzerland
[b] Faculty of Civil Engineering and Geosciences, Delft University of Technology, Stevinweg 1, 2628 Delft, The Netherlands

ABSTRACT

This paper presents a formwork system consisting of a bending-active gridshell that simultaneously serves as falsework and integrated reinforcement for realising a ribbed funicular concrete skeleton shell. Encased by a knitted textile shuttering, the formwork system was demonstrated through KnitNervi, an architectural-scale, funnel-shaped demonstrator measuring 9 m in diameter and 3.3 m in height. The gridshell is materialised from straight steel rebar actively bent into curvilinear, double-layered rebar cages. Regular stirrups and pairs of inclined stirrups forming triangulated shear connectors provide the necessary shape control and stiffness for the load-bearing falsework. The rebar cages define the shape of the concrete ribs by supporting a knitted closed sectional mould and stay in place to structurally reinforce the resulting ribs.

The focus of this paper lies on the falsework and reinforcement system with its interrelated design drivers. The geometric design includes the funicular form finding of the target shell with Thrust Network Analysis and the incremental form finding of the bending-active gridshell with its informed assembly sequence towards the funicular target with Finite Element Analysis. The engineering of the falsework demonstrates its sufficient load-bearing capacity and deflection control to support the weight of the wet concrete at an architectural scale. Sensitivity studies reveal the effectiveness of activating the double layer through the shear-connecting stirrups, the relevance of the internal connection design, and the geometric integrity during a potential stepwise casting sequence. The construction of the demonstrator verified the shape control and fabrication design.

In only 36 h, the bespoke falsework gridshell was efficiently assembled from its kit-of-parts of standard rebar elements with adequate precision, logistics, time, and material resources. It was relatively lightweight, compact for transport, and employed low-tech construction techniques common to the rebar industry. Its structural geometry and informed bending-active logic enabled its efficient construction without digital fabrication or wasteful, costly moulds, which typically present the bottleneck for custom concrete structures. The resulting funicular concrete skeleton shell saves structural mass, hence embodied carbon, compared to unarticulated bending-dominant typologies. The overarching motivation of the research is to outline a strategy that could mitigate the environmental impact of the construction sector, applicable to a broad range of technological contexts.

1. Introduction

1.1. Motivation

The concrete industry is responsible for tremendous shares of the world's human-made carbon dioxide emissions, energy consumption, and material depletion [1]. Inexpensive and accessible, reinforced concrete (RC) is the most widespread construction method [2], with spanning structures accounting for the largest part of the building mass [3]. Even though concrete's moldability allows it to take on virtually any shape, it is commonly used in highly inefficient beam and slab typologies where only a fraction is structurally activated in bending. In contrast, funicular shells obtain their strength through their structural geometry rather than material strength [4]; their cross-section is fully

activated in compression. Structural articulations that increase structural depth, such as stiffening ribs, enhance material efficiency further [5]. Consequently, the structural material quantity is reduced, which is a highly effective strategy for reducing embodied carbon besides modifying the material composition [6].

Advances in computational engineering make the form finding, design, and analysis of funicular shells more accessible [7]. However, the materialisation of bespoke geometry typically requires complex manufacturing methods. Conventional formwork strategies for non-standard construction are costly, waste-intensive, and bound to digital fabrication facilities [8,9]. Moreover, their reinforcement is complex and tedious, typically requiring intensive manual labour and inefficient transport for prefabricated elements. This often remains a bottleneck even in innovative formwork solutions, such as 3D printing or flexible formworks [10,11].

This paper presents research into a construction system that unifies the reinforcement and formwork into one structural stay-in-place formwork and bases its efficiency for both the formation and resulting structure on its structural geometry. The proposed flexible formwork system consists of (i) a bending-active gridshell made from rebar elements that serves as falsework, supporting the shuttering and wet-concrete weight, and stays in place as integrated reinforcement, and (ii) a stiffened knitted textile shuttering that encases it, allowing concrete to be cast into. It is designed to enable the construction of a ribbed funicular concrete skeleton shell. Consequently, the proposed formwork and reinforcement solution aims to be material-efficient, lightweight, compact for transport, and not dependent on high-tech fabrication. The research's overarching motivation is to enable a material-efficient, waste-free construction method of a material-efficient structure and hence to outline a possible strategy that aims to mitigate the environmental impact of the construction sector.

1.2. State of the art

Funicular shell structures typically are compression-only and limited to vault-like geometry. By introducing a circumferential funicular tensile ring, their horizontal thrust can be contained. This enables funnel-shaped funicular structures with free, lifted boundaries and expressive geometries. These can be materialised as continuous shells, with stiffening ribs or as ribbed skeletons. Their broadened design space was explored in the pioneering work of Rippmann and Block [5].

Such funicular structures can be form found for their dominant load case using Thrust Network Analysis (TNA). It enables a graphical exploration of statically indeterminate, highly shape-constrained systems based on principles of 2D graphic statics extended to compression-only 3D structures [12]. To broaden the design space to such expressive funnel shapes, TNA was extended to tensile members by reversing edge orientations to close the force diagram, allowing overlapping edges and non-convex polygons [13]. The algorithm is implemented in COMPAS, a Python-based, open-source framework for research in computational architecture, engineering, and construction [14], in the compas_tna package [15].

Likewise, to the geometric efficiency of shells, flexible formworks rely on their geometric stiffness and thus are material-efficient and lightweight. They utilise tensile or bending-active structural systems as falsework. The tensile flexible formwork systems KnitCandela (Fig. 1a) and NEST HiLo [11,16] consist of lightweight mechanically-prestressed cable-net falsework and fabric shuttering. However, because of their high prestress, their shapes are limited to anticlastic curvature, and they require stout boundary frames. If non-optimised, the latter can result in approximately 75% and 45% of the construction's cost and time, respectively [16].

The textile shuttering can be manufactured using the CNC-knitting technology KnitCrete [17]. It offers custom features such as bespoke density patterns and sleeves. Together with pneumatic cushions, this enabled a cross-sectional articulation in the KnitCandela shell [16].

Fig. 1. Selected references: (a) Tensile flexible formwork, KnitCandela, Mexico City, 2018 [16]; (b) Bending-active flexible formwork Lift-Shape [23]; (c) Bending-active flexible formwork with corrugation [21]; (d) Integrated formwork for ribbed RC shell, Palazzetto dello Sport, Rome, 1957 [29]; (e) Combined falsework and reinforcement, National Theatre Taichung, 2014 [30]; (e) Combined falsework and reinforcement, Mesh Mould [31].

However, the knit must be stiffened with mortar or epoxy resin to withstand the wet-concrete load and hydrostatic pressure [17,18].

Active bending is the deliberate elastic deformation of slender, initially straight elements into 3D curved geometries without the necessity for formworks [19]. In contrast to tensile falsework, flexible formworks with bending-active falsework allows for both anticlastic and synclastic curvature and reduced boundary conditions by self-containing the active-bending reactions [20,21]. Various explorations on bending-active falseworks with textile shuttering were carried out. Winn [22] demonstrated the construction of a concrete hangar using a bending-active gridshell falsework, and Marsh [23] invented the Lift-Shape method, a deployable gridshell serving as concrete falsework (Fig. 1b). Tang and Pedreschi [24] investigated the reconfigurability of a reusable gridshell falsework, while Cuvilliers et al. [20] investigated a composite system where the gridshell stays in place as external reinforcement. Popescu et al. [21] used separate splines in a tensile hybrid system instead of a gridshell (Fig. 1c), and Shah and Irani [25] proposed a low-tech reusable gridshell falsework for vaulted floors.

However, most single-layered explorations are limited in scale as they suffer the dilemma of requiring flexibility for the formation and stability for the structural performance. Thus, bending-active gridshells often consist of two slender layers that are shear connected after their erection to increase the static height and lock the shape while allowing greater curvature than a single thicker layer [26].

The bending-active falsework examples are also limited in shape control, as a bending-active gridshell is a form-active structural typology. Hence its form must be found through its static equilibrium with bending stresses and cannot be forced into any shape [19]. Its form finding can be performed with Finite Element Analysis (FEA) to simulate the mechanical behaviour and potential instabilities. The SOFiSTiK software [27] provides a built-in function that computes internal bending stresses based on the initially straight, unstressed states of a curved input geometry. These stresses drive the system from its ideal, starting geometry to equilibrate with geometric nonlinear, third-order analysis into its deformed form-found shape. The geometric outcome and stress state is identical to a simulation that commences with straight

splines that are actively bent in with contracting cables [28].

In most flexible formwork approaches, the integration of internal reinforcement with sufficient concrete coverage remains a bottleneck. However, when the falsework is materialised from rebar and integrated into the concrete, the falsework can stay in place to serve as integrated reinforcement. A historical example is Ferrocement, used by Pier Luigi Nervi in the Palazzetto dello Sport (Fig. 1d), where rebar and mesh wire served for prefabricated moulds [29]. As falsework integration, it was demonstrated in the National Theatre Taichung by Toyo Ito with highly dense reinforcement and an additional textile shuttering layer creating a closed mould (Fig. 1e) [30] and in the robotically-fabricated Mesh Mould without shuttering, limiting it to vertical elements (Fig. 1f) [31].

The bending-active formwork explorations by Winn [22] and Marsh [23] also integrated the bending-active falsework as stay-in-place reinforcement. However, the concrete must be applied incrementally onto these open, single-sided formworks that create surface structures without cross-sectional articulations. The only bending-active formwork with cross-sectional articulations was created by Popescu et al. [21] through stiffening corrugations (Fig. 1c). None of the bending-active formwork systems combines measures for structural performance at larger scales, shape control, integrated reinforcement, structural articulations, and closed moulds.

1.3. Research objectives

The overarching objective of this research is to design a formwork system that allows the efficient formation and reinforcement of a material-efficient structure, a funicular concrete skeleton shell. The proposed system aims to address the falsework challenges identified in Section 1.2 and to build upon the advantages and opportunities of different strategies by combining these into one formwork system. Hence, the resulting research questions for a bending-active formwork system are as follows:

- How can the formwork system be designed and detailed such that the falsework structure can simultaneously serve as integrated reinforcement with sufficient concrete coverage and such that it provides a spatial substructure that supports a closed-mould shuttering for shaping the concrete skeleton? (Section 2)

- How can the shaping of the bending-active gridshell falsework from initially straight bars be controlled towards a funicular target shape with syn- and anticlastic curvature? (Section 3)
- How can the gridshell falsework be engineered and detailed such that it is sufficiently flexible for its formation and perform with sufficient load-bearing capacity and deflection limits to support the weight of the wet concrete at an architectural scale? (Section 4)
- How can the falsework be realised on-site efficiently and pragmatically such that these challenges of system design, shape control and stiffening strategies are satisfied with adequate precision, logistics, time, and material resources? (Sections 5 & 6)

Consequently, this paper focuses primarily on the design, engineering, and construction of the bending-active gridshell that serves as falsework and integrated reinforcement. A separate publication will present the knitted shuttering with its pattern design, fabrication and assembly logic.

1.4. System concept

To address the challenges of the research objectives, the proposed formwork and reinforcement system is based on the following concepts (Fig. 2). To both define a controlled doubly-curved shape and structurally support the wet-concrete weight, the lightweight falsework is realised as a double-layered bending-active gridshell with shape-controlling crossing connections and shear-locking stirrups. To integrate the falsework as reinforcement and to generate a closed mould for skeleton ribs, the falsework is materialised from rebar splines that are actively bent into rebar cages. These generate the basis for the cross-sectional shape of the ribs of the skeleton shell. Contrary to typical concrete construction, where the formwork supports spacers that position the reinforcement with minimal concrete coverage, here, the order is reversed such that the reinforcement supports spacers to position the shuttering. The shuttering consists of a taut flexible knit that is impregnated with resin to provide a stiff mould. It encloses the gridshell forming a closed mould to shape the reinforced-concrete ribs, in which the gridshell stays-in-place and is structurally-integrated as their reinforcement.

Fig. 2. A typical node of the proposed construction system during the different construction stages (from left to right): actively bent rebar cage with stirrups as gridshell falsework; plastic rebar spacers, supporting shuttering rods; flexible knit shuttering; resin impregnation for stiffening; and concrete cast integrating the falsework as stay-in-place reinforcement.

1.5. KnitNervi at MAXXI

The proposed formwork system was demonstrated on an architectural-scale demonstrator named KnitNervi (Fig. 3), which was part of the exhibition *Technoscape – the Architecture of Engineers* [32]. The demonstrator was located in the courtyard of the MAXXI Museum in Rome, Italy, from June 2022 to April 2023. KnitNervi derived its name from the knitting technology employed for the textile shuttering [17] and from the master builder Pier Luigi Nervi as it drew inspiration, as a homage, from the iconic and pioneering Palazzetto dello Sport (Fig. 1d) [29], located in the close vicinity of the museum.

As the focus of this research lies on the formwork system and in order to limit construction demolition waste for a temporary pavilion, the KnitNervi demonstrator omitted the knit-impregnation and concrete-casting steps. Besides, the engineering and realisation of the concrete structure can be considered common practice and would not result in novel research contributions. The pragmatic feasibility of the impregnation and casting steps were tested in a prototype of a typical node (Fig. 2), and the structural impact of the wet-concrete weight was investigated with structural simulations (Section 4).

The KnitNervi demonstrator (Fig. 3) had a funnel geometry such that it would be funicular for the concrete skeleton shell subject to dead loads. The structure was circular in plan with a horizontal circumferential tensile ring with a diameter of 9 m at a height of 2.8 m. An inner compressive droplet-shaped oculus provided partial ground support and was also circular in plan with a diameter of 3.5 m. A diagrid of compressive prismatic ribs spanned between the boundary rings, which contained their horizontal thrust as in [5]. The ribs created a ribbed funnel shell of synclastic and anticlastic curvature with a maximum height of 3.3 m. The structure's surface of 65 m^2 covered an area of 56.6 m^2 in plan.

The primary analogy of KnitNervi to the Palazzetto dello Sport lies in its circular plan and diagrid of prismatic concrete ribs, primarily subject to compression. Furthermore, likewise to Nervi's use of Ferrocement for enabling such articulated geometry [29], the proposed system utilises the reinforcement as falsework. However, instead of Nervi's limitation to repeated units, KnitNervi aims to open up the design space to structures of custom, varying curvatures. Hence, it enables the materialisation of a structure that draws inspiration from the expressive funicular funnel geometries by Rippmann and Block [5]. KnitNervi is equally a design descendent and homage to these innovators, while it also deliberately resembles the soap film explorations by Frei Otto [33], materialised in the Stuttgart main station [34].

1.6. Co-design methods and specific technical objectives

The system design (Section 2) is the result of its geometric design (Section 3), structural design (Section 4) and fabrication design (Section 5), which are inseparable and reciprocal design drivers. In addition, the integrated formwork system and the concrete shell constitute only different construction stages of one construction system, as one serves to shape the other. Hence, they are geometrically, structurally, and fabrication-wise directly interrelated, even though their structural behaviour differs fundamentally. Thus, the system design must be approached with a nonlinear co-design process that integrates these interdependent constraints (Fig. 4).

The design workflow was implemented in the COMPAS framework [14]. A design-to-fabrication modelling workflow with a custom assembly graph data structure was developed to handle the complex topology and geometry of the double-layered gridshell with its connectivity and dependencies to other elements of the construction system throughout the construction stages [35].

The global geometric design is determined with funicular form finding using Thrust Network Analysis (Section 3.1). Informed by the structural behaviour of both systems, the structural shape is translated to the topological and cross-sectional design of the interrelated gridshell build-up and concrete ribs. In response to the shape control objective, the bending-active gridshell's geometry must be controlled from the Elastica shape towards the funicular target through the diagrid and stirrup connections (Section 3.2). The specific technical objective is to derive an informed assembly sequence of the gridshell, such that the deviations to the target shape decrease while revealing the importance of the crossing positions and stirrup connections of the double layer. The bending-active form finding and its structural design are performed with the FEA-software SOFiSTiK.

The falsework must withstand the wet-concrete load with sufficient load-bearing capacity and within defined deflection limits as the deformations result in geometric imperfection in the ribbed shell. The gridshell will be analysed under various load conditions (Section 4.1) in terms of its structural behaviour in general and specific to the double layer and boundary rings (Section 4.2). In response to the stiffness-control objective, the specific technical challenge is to detail effective
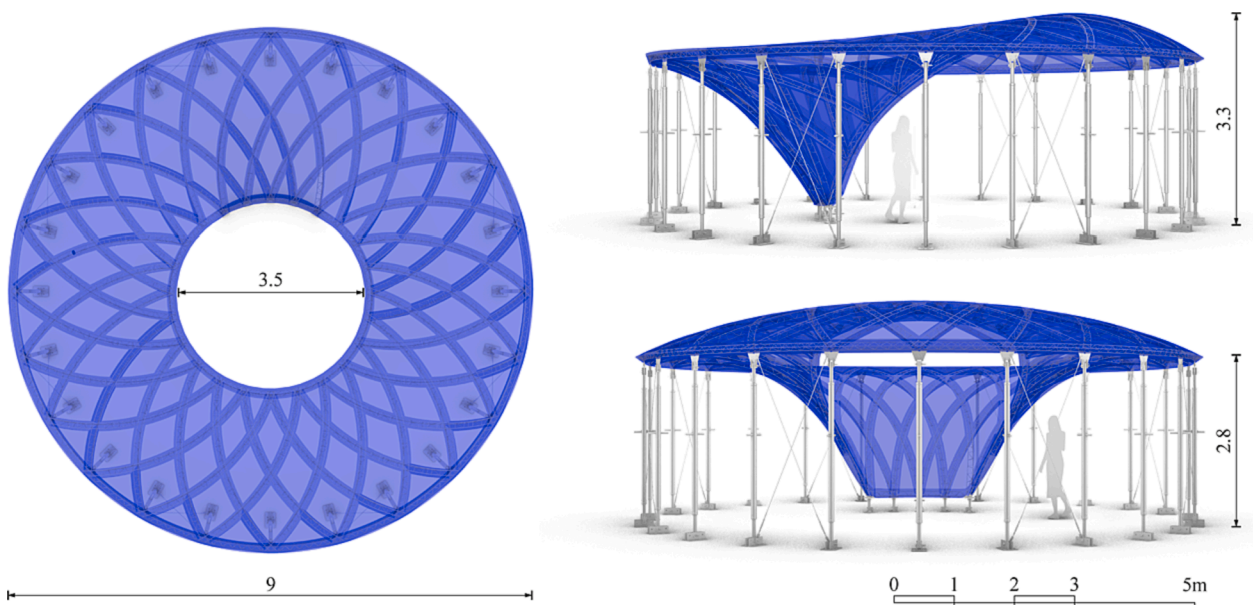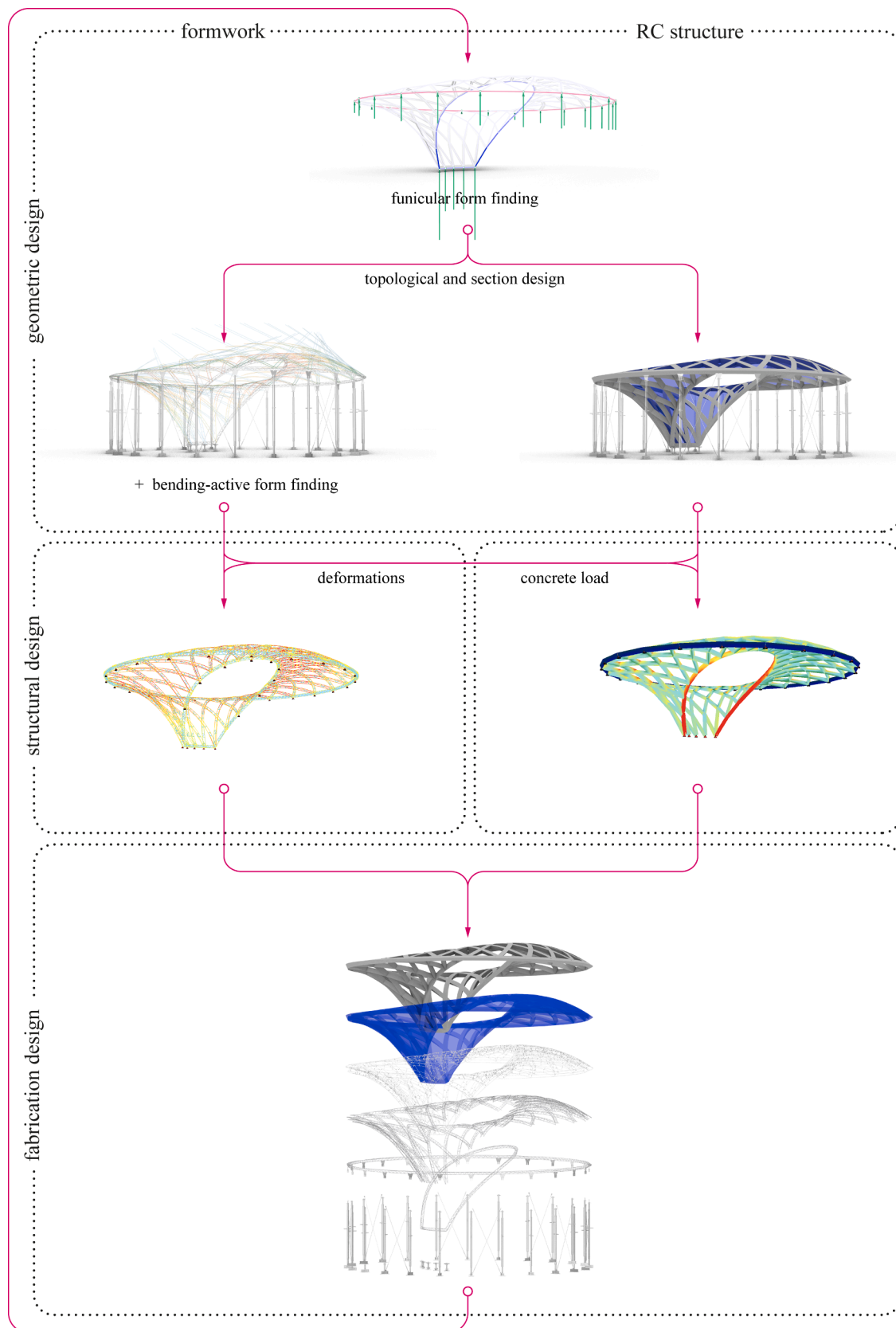

Fig. 3. Plan, side elevation, and front elevation of the KnitNervi demonstrator with main dimensions in metres.

Fig. 4. Workflow of the co-design of the integrated geometry, structure and fabrication for both the integrated falsework system and reinforced-concrete shell.

crossing connections within the splines and shear connections within the layers. Sensitivity studies reveal the impact of the stirrup types and their placement density on the activation of the double layer (Section 4.3), demonstrate the relevance of the internal connection design in terms of connection stiffness (Section 4.4), and investigate the geometric integrity during a stepwise casting sequence (Section 4.5).

In response to the gridshell's shape-control objective for the fabrication design, the specific technical challenge is to translate the simulation steps (Section 3.2) into a clear on-site assembly sequence (Section 5.1). In return, the process decisions reinform the numerical form finding. In response to the pragmatic realisation objective, the specific technical challenge is to validate whether the prefabrication and on-site assembly process is feasible pragmatically and with reasonable logistics (Section 5.3). Geometric measurements serve as guidance and evaluate the precision (Section 5.4).
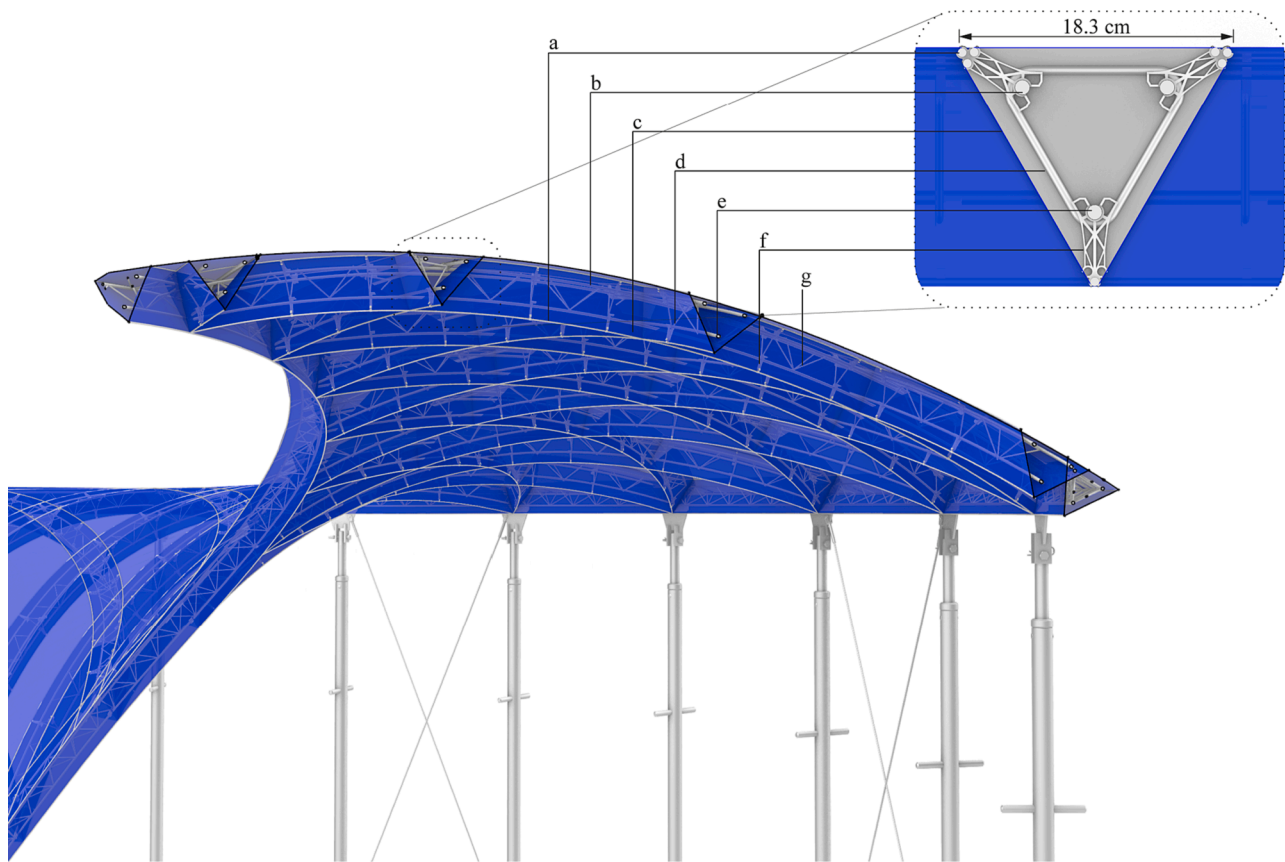
2. Construction system

The proposed construction system consists of standard scaffolding props (Fig. 5a) that support prefabricated gridshell boundary rings (Fig. 5b) in between which the gridshell ribs are actively bent (Fig. 5c). This rebar cage supports spacers that clip in slender shuttering rods (Fig. 5d), that form crisp edges of the knitted shuttering (Fig. 5e), into which, in principle, after stiffening the knit, the concrete ribs could be cast (Fig. 5f). Together, these elements form prismatic ribs with an equilateral triangle cross-section with side lengths of 18.3 cm as shown in Fig. 6.

2.1. Scaffolding

Pin-ended struts prop the outer ring permanently and the inner ring temporarily during construction by taking vertical reactions from permanent loading. These are materialised as conventional, reusable, telescopic steel scaffolding props. Steel cable crosses, pretensioned with
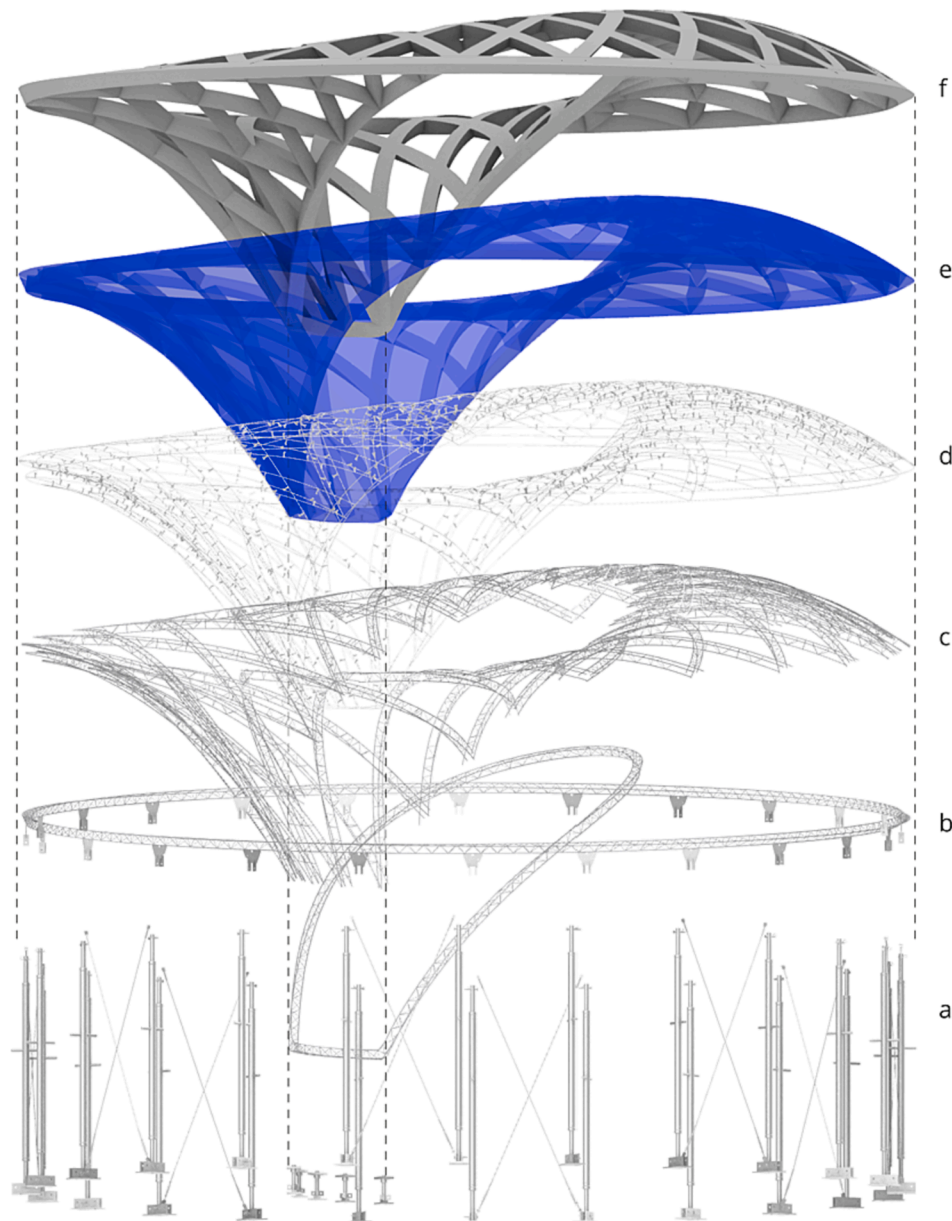
Fig. 5. Exploded view of the construction system showing (a) reusable scaffolding props with bracing, (b) prefabricated boundary gridshell rings, (c) bending-active gridshell ribs, (d) spacers and knit splines, (e) stiffened knit shuttering, and (f) concrete ribs.

Fig. 6. Closeup of the construction system showing concrete cross-section with (a) double-layered bending-active gridshell with (a) shuttering edge rods, (b) pair of upper splines, (c) textile shuttering, (d) distancing stirrups, (e) lower spline, (f) custom plastic spacers, and (g) bracing stirrup pairs.

turnbuckles and positioned in every third bay along the perimeter, provide lateral stiffening for wind loads (Fig. 5a).

2.2. Gridshell boundary rings as falsework and reinforcement

The two rings serve as load-bearing and shape-defining boundary conditions of the gridshell (Fig. 5b). They are prefabricated and discretised into six segments for the outer ring and three segments for the inner ring. The segmentation size is based on handling and transport constraints, and the segmentation position is informed by structural constraints. Unlike the massive boundary beams of the tensile cable-net fabric formwork systems [11,16], the rings are made from the same rebar elements and with identical cross-sectional dimensions as the gridshell ribs (Section 2.3) and equally serve as falsework and reinforcement. Instead of the inclined stirrups, continuous bracing forms a triangulated lattice girder to lock the shape and provide higher stiffness. Additionally, spline segments with threaded ends are connected to the rings to provide connections for the rib splines.

2.3. Gridshell ribs as falsework and reinforcement

The initially-straight splines are shaped into the curved geometry, controlled solely by their lengths and crossing positions. The gridshell's rib cross-sections are composed of a trio of splines each, with a pair in the upper layer and a single spline in the lower layer (Fig. 5c, Fig. 6b&e). The triangular cross-section provides a double-layered rib in the shell plane and out-of-plane. To provide sufficient stiffness and shape control for the self-supporting, load-bearing falsework, the two layers are connected with two types of stirrups, referred to as bracing and distancing stirrups. Pairs of inclined, triangulating stirrups shear-connect the two layers to activate the full structural depth and lock in the gridshell's

shape (Fig. 6g). However, the inclined stirrups do not define the spacing of the two layers as their relative inclination is impractical to measure during construction. Consequently, additional regular orthogonal stirrups (Fig. 6d) are required to maintain a constant spacing between the longitudinal rebar splines. These define the distance during construction through their orthogonality requirement and hence contribute to the global system's shape control (Section 3.2). Furthermore, they provide rotation supports for the spacers (Section 2.4), which cannot click onto the inclined stirrups. Together with the longitudinal splines, the stirrups create the rebar cage that stays in place and reinforces the concrete ribs in which the stirrups provide shear reinforcement as in conventional linear concrete elements.

The gridshell falsework is materialised from conventional steel rebar with a diameter of 10 mm for the splines and 6 mm for the stirrups. The splines' diameter is determined by the maximum elastic bending curvature and actuation force within the strength limits of a construction worker. The smallest industry-standard rebar defines the stirrups' sizing. The mechanical properties of reinforcement steel B500 lie just in the suitable range for active bending with high strain and flexural strength [19]. Unlike conventional bending-active materials such as timber or fibre-reinforced polymers, the high plasticity of steel permits the forming of stirrups.

The splines are connected within the diagrid crossings and to the stirrups with metal tie wires using cross ties commonly used for main rebar connections that must withstand high forces. The spline's ends are threaded and connected to the ring's spline segments with hexagonal connecting nuts M10 × 30 mm fixed with a regular M10 nut on each side. These are conventional techniques in rebar industry.

2.4. Spacers

A customised rebar spacer made from plastic is clipped onto each longitudinal spline rebar at each distancing stirrup corner (Fig. 6f). Their design is modified from conventional stay-in-place plastic circular wheel spacers. It provides an additional clip for the shuttering shaping rods at its extremity and a rotation detent to the distancing stirrups preventing distortion of the shuttering triangle to ensure minimum concrete coverage. The plastic spacers are produced with fused deposition modelling additive manufacturing; for greater production output, their design would allow injection moulding.

2.5. Knitted textile shuttering

The knitted shuttering made of polyester yarn is composed of separate rib and surface strips with sleeves along their edges. Slender metal shuttering rods (Fig. 5d & Fig. 6a) are introduced into the sleeves and clipped into the spacers to position and tauten the shuttering (Fig. 5e & Fig. 6c) with crisp edges around the falsework. The KnitCrete technology [17] offers such custom sleeves through digital fabrication. Alternatively, off-the-shelf industrial fabric can be utilised where the sleeves are sewn in a low-tech manual process or with CNC-sewing machines. In both cases, the flexible fabric is not sufficiently stiffened by double-curvature or mechanical prestress and must be stiffened with epoxy resin to shape crisp concrete cross-sections while withstanding the hydrostatic pressure of the concrete. The shuttering can be removed or stay in place as a lost formwork serving additional functions.

2.6. Concrete ribs

The concrete diagrid ribs (Fig. 5f) would integrate the rebar splines resulting in a longitudinal reinforcement degree of 1.4%. The constructional design is closely oriented along constructional standards for primarily compressive bars. It deviates in lower reinforcement degree, stirrup density, and rebar diameter, as it is a primarily funicular structure. However, the flexural reinforcement of the longitudinal splines with stirrups is crucial to provide bending resistance for non-funicular live load cases. The tensile outer ring would require post-tensioning to avoid concrete cracks and activate the concrete section.

In open, single-sided moulds of flexible formworks for continuous shells, the concrete is applied in thin layers to distribute the wet-concrete loads evenly [16]. In contrast, the closed rib moulds would require the full casting of the cross-sections due to their limited accessibility. However, the casting must be performed stepwise to limit the wet-concrete's hydrostatic pressure onto the textile shuttering and spacers. The geometric and structural impact of the non-distributed loading during the casting sequence on the gridshell falsework is structurally investigated in Section 4.5. The casting is not performed in the demonstrator; nevertheless, the stepwise casting could be conducted by inserting a slender concrete pump hose from openings in the textile shuttering at the outer ring through the centre of the rebar cage down to its respective concreting segment and by pulling it up incrementally following the concreting sequence.

3. Geometric design

### 3.1. Form finding of the funicular target geometry

The global geometric design of the funicular funnel structure is determined with funicular form finding using the extended TNA implementation that allows for tensile members [15]. In TNA, the horizontal equilibrium is achieved graphically and then the vertical equilibrium is computed through successive linear equilibrium problems with an iterative numeric force density solver updating the self-weight to respond to the changing tributary areas until convergence [36]. For this research project, the computation of the self-weight was modified for a load distribution of a ribbed skeletal shell instead of a continuous shell, which results in a maximum deviation of 8 cm in the resulting 3D shape [35].

The KnitNervi's pattern is inspired by Rippmann and Block [5] and is essentially an evolution from the pattern of Nervi's Palazzetto dello Sport (Fig. 7a) with the following differences: a smaller dimension from a diameter of 61 m down to 9 m and less resolution in the diagrid down to 48 ribs (Fig. 7b); the buttress system at the perimeter is replaced by a tensile ring to equilibrate the horizontal thrust resulting in vertical-only supports (Fig. 7c); there is a proportionally larger and open central oculus that is partially vertically supported on the ground (Fig. 7d).

In the TNA analysis, the pattern is taken as input for the form diagram **Γ** (Fig. 8a), the horizontal projection of the ribbed skeletal shell. Through the horizontal equilibrium, the force diagram **Γ*** (Fig. 8b), the horizontal force polygon that indicates the magnitude of forces, becomes perpendicular, thus reciprocal. The tension ring creates a self-stressed
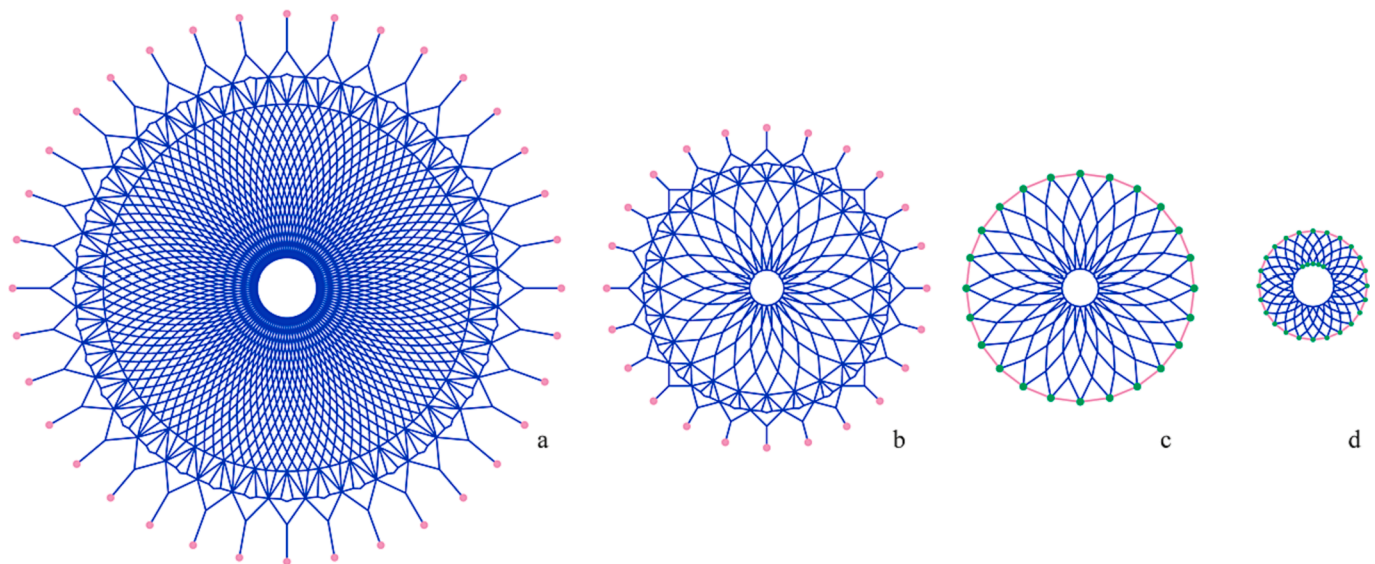
Fig. 7. Evolution of pattern from (a) the Palazzetto dello Sport with horizontal-thrust taking supports (pink) to (b) reduced scale and resolution to (c) tension tie (pink) with vertical-only supports (green) to (d) proportionally larger oculus with partial vertical-only supports (green). (For interpretation of the references to colour in this figure legend, the reader is referred to the web version of this article.)
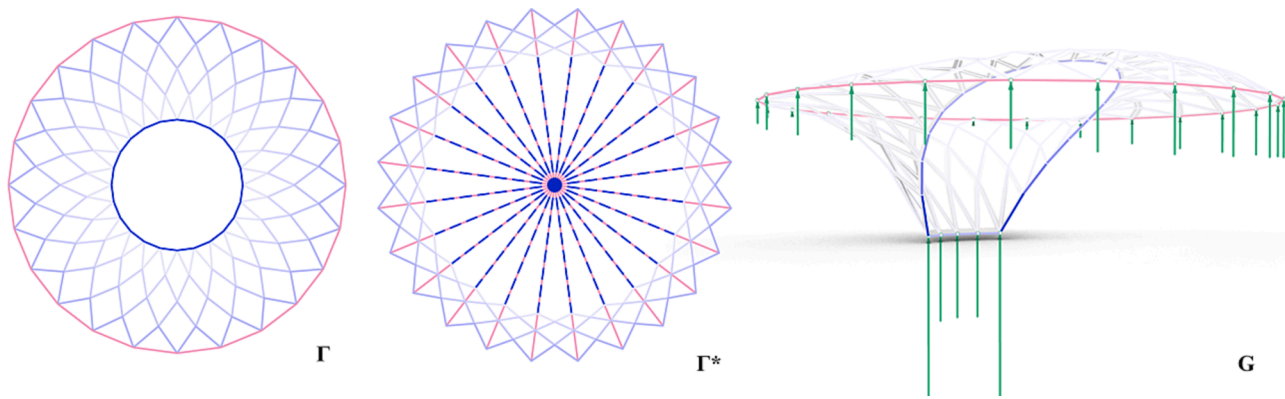
Fig. 8. Form diagram **Γ**, force diagram **Γ***, and thrust network **G** for the funicular shell geometry with circumferential tensile ring (pink), compressive oculus ring and diagrid ribs (with forces in a gradient of blue), support reactions (green), and tributary areas for self-weight calculation of ribbed shell (white). (For interpretation of the references to colour in this figure legend, the reader is referred to the web version of this article.)

system. As a consequence, only vertical support reactions will arise in the vertical equilibrium.

The structure is rotationally symmetric in its horizontal projection. All rib edges in the same hoop have the same magnitude of horizontal force that decreases slightly towards the centre. The tensile forces in the outer ring and compressive forces in the inner ring are significantly larger. The convex opening in the form diagram **Γ** reflects in a spoke wheel-shaped topology in the force diagram **Γ***. The same applies to the tensile ring at the outer boundary, which can be interpreted as an inverted opening [5]. Both spoke wheels overlap in the force diagram **Γ*** (dashed line).

The vertical equilibrium results in an axis-symmetric thrust network **G** (Fig. 8c), the spatial representation of the shell. Its tensile ring forces are identical to their horizontal projection **Γ**, as there is no vertical force component. However, in its compressive ribs and ring, the forces increase towards the centre ground supports as the vertical component increases the steeper the edges.

The minor modifications in the input pattern from the Palazzetto dello Sport caused significant variations in the 3D shape and its spatial articulation. The resulting self-stressed system dispenses the need for buttressing such that the perimeter of the shell can be lifted from the ground. Moreover, through the partial central supports, a funnel with droplet-shaped oculus emerges. The topology and cross-section design of spline trios and prismatic ribs translate the resulting funicular shape into the construction system (Fig. 6).

3.2. Form finding of the bending-active gridshell

The FEA input model of the bending-active gridshell (Fig. 9) is generated with a custom interface from COMPAS to SOFiSTiK based on the assembly graph data structure [35]. It enables modelling continuity
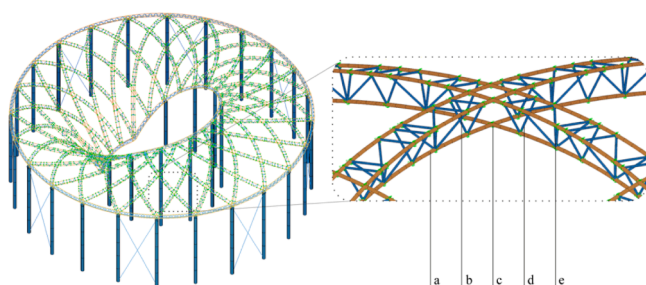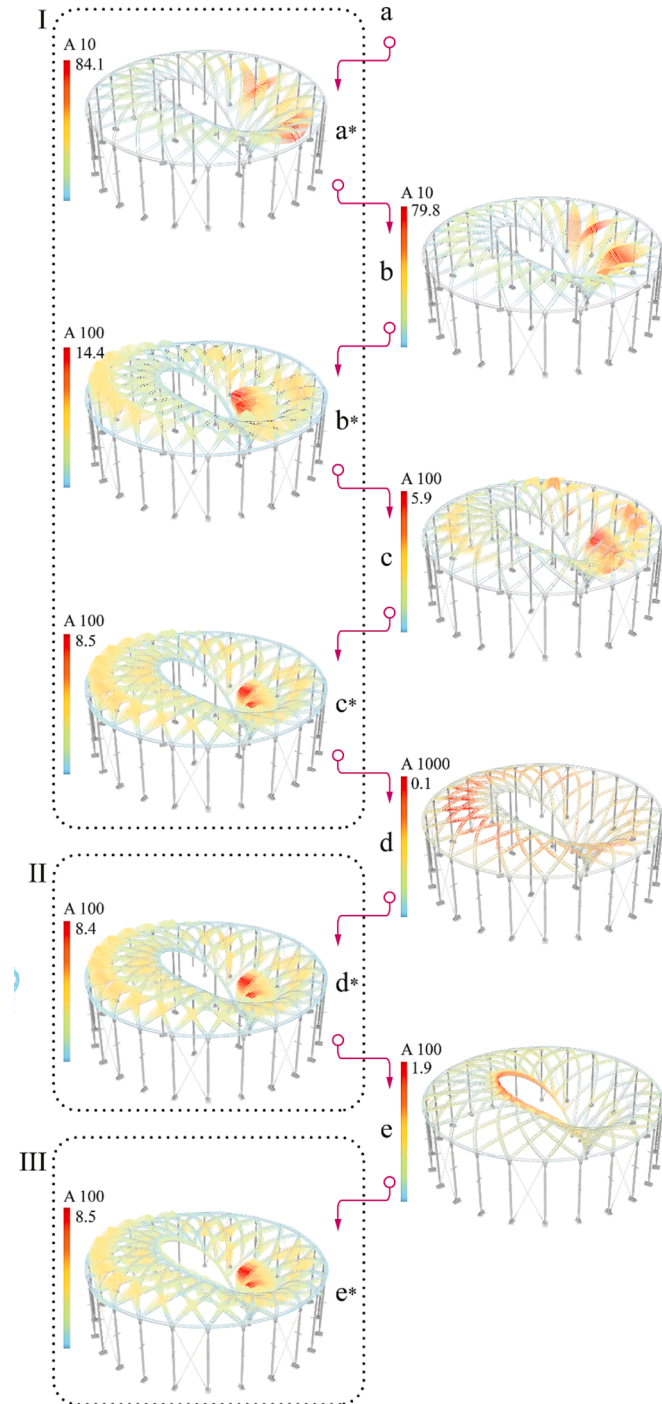
within the steel splines and explicit hinge conditions with zero-length springs or rigid couplings connecting the spline layers amongst themselves and to the stirrups. The model takes as input the material, sectional values, and connectivity described in Section 2.3. The props are pinned, and the cables are pretensioned by 8 kN for lateral bracing against wind loads (Section 2.1). Additional stiffness that could be provided by the impregnated knit is not taken into account.

The objective of the form finding of the bending-active gridshell is to control the shape of the initially straight bars towards the funicular target shape with syn- and anticlastic curvature. Using the function and procedure by Bellmann [28] (Section 1.2), the form-finding procedure commences from the ideal funicular target geometry and finds equilibrium with induced internal bending stresses. However, if the model contained all elements in their ideal target geometry, minimal deformations would occur because the stirrups would lock the geometry. Consequently, the form finding relies on an incremental build-up process. In each step, the results are deviations **Δ** from the funicular target and the differences between these deviations **Δ** are the deformations **δ** caused by the respective assembly step. The incremental process is structured into three phases - (I) the formation phase, starting from the Elastica splines, which are subsequently connected at their crossings, and subsequently connected with the second layer by the regular stirrups, while the inner ring is temporarily propped; (II) the geometric locking phase, by adding the bracing stirrups; and (III) the boundary conditions adjustment phase, by releasing the inner ring. This is informed by the assembly sequence (Section 5.1) and informs it vice versa.
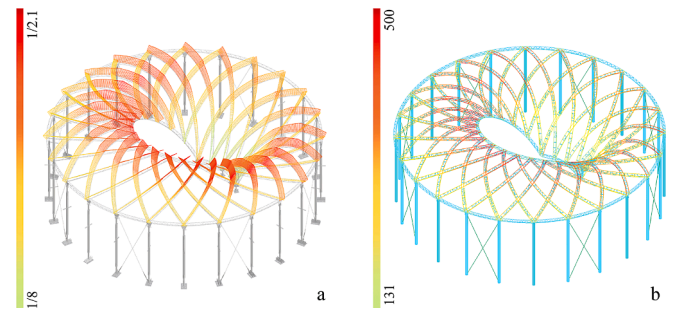
In (I) the formation phase, where the bending-active gridshell is manipulated towards the funicular target geometry, the major control parameters are the spline lengths, their crossing positions and their connection to the second layer. When the initially-straight splines are only anchored at their ends to the rings with a bending-stiff connection, they deform separately into Elastica shapes. This Elastica geometry deviates by 84.1 mm from the ideal funicular target geometry (Fig. 10a*). When the splines are connected at their target crossing positions, the geometry is refined tremendously towards the target to deviations **Δ** of 14.4 mm (Fig. 10b*). Connecting the crossing splines requires forces of maximal 0.3 kN and induced additional internal bending stresses of 113 MPa. When the upper and lower spline layers of the gridshell are restrained with the distancing stirrups to a constant spacing, the equilibrium shape approaches the target further with a maximum deviation **Δ** of 8.5 mm (Fig. 10c*). In the physical process, the position of the spline connections can be controlled by crossing marks, and the distance between the layers can be controlled by the orthogonality requirement of the distancing stirrups.

In (II) the locking phase, the bracing stirrups are added to shear-connect the two layers and thereby lock the form-found shape. Besides

Fig. 9. FE-model of the double-layered gridshell with (a) continuous lower spline, (b) continuous upper spline pair, (c) connection by zero-length spring or rigid coupling with rotational hinge condition, (d) distancing stirrup, and (e) bracing stirrup pair.

adding self-weight, the bracing stirrups do not modify the shape as their relative connection position of the upper to the lower layer is not prescribed in the physical process. They are only activated in (III) the phase of the boundary adjustment, where they stiffen the structure such that the inner ring only moves 1.9 mm upwards (Fig. 10e). The resulting form-found shape of the gridshell deviates by 8.5 mm from the funicular target shape with a higher curvature in the back area close to the

Fig. 11. Results from FE form finding of the bending-active gridshell with (a) spline curvature in comparison in 1/m to (b) spline stresses in MPa.

supports and less curvature in the top area (Fig. 10e*). And the stresses of the form-found shape compared to the ideal funicular geometry deviate by 87 MPa.

The splines' stresses predominantly result from the active bending and hence are directly related to their curvature graph (Fig. 11, compare a to b). The highest stresses and curvature occur extremely locally in the top splines close to the inner ring; these stresses are expected to relax over time. The maximum allowable curvature κ or minimum bending radius R_{min} is determined by $\kappa = 1/R_{min} = f_y/(E\ d/2)$ to 1/2.1 m with the diameter $d = 10$ mm, yield strength $f_y = 500$ MPa, and Young's modulus $E = 210$ GPa for reinforcement steel. It is equivalent to a bending moment $M = 0.049$ kNm with $M = EI\ \kappa = EI/R_{min}$.

4. Structural design

4.1. Load cases

To demonstrate that the gridshell falsework performs with sufficient load-bearing capacity and serviceability, it must withstand the temporary wet-concrete load, wind loads, and live loads, besides its permanent loads with internal bending stresses. Five load cases (LC) are considered: LC1 is the wet-concrete load case with 0.32 kN/m along the ribs, resulting in a total of 70 kN for a specific weight of 20 kN/m³ (Fig. 12a). In Section 4.2, the wet-concrete load is simplified to be applied at once; for the impact on the casting sequence, refer to Section 4.5.
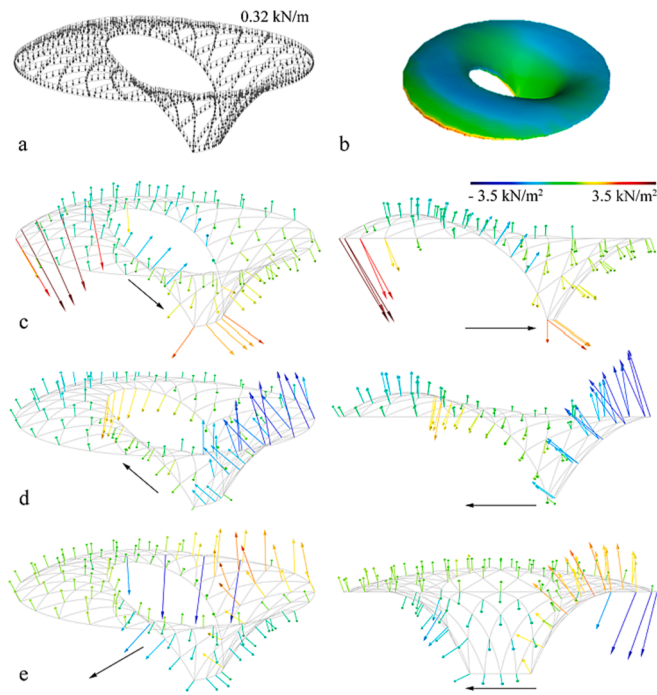
LC 2 is a maintenance load case of 1 kN in the most critical position, the back area, where the double curvature is minimal. LC3 to LC5 are wind load cases from the front (Fig. 12c), back (Fig. 12d), and side (Fig. 12e); three, as the structure is axis-symmetric. No standard shape from the Eurocode was applicable for the pressure distribution on the complex geometry. Thus, computational fluid dynamics simulations (Fig. 12b) were conducted based on a wind speed of 27 m/s (EN 1991-1-4). The sums of the resulting upper- and underside pressure values were scaled to comply with comparable Eurocode distribution values for a conservative assumption. Since the scaffolding and KnitNervi demonstrator are temporary structures, the wind loads can be reduced by 50%. All loads are safety factorised for the ultimate limit state. Only for the concrete load case LC1 the inner ring is temporarily propped.

4.2. Structural analysis

The structural analysis reveals the structural behaviour of the gridshell with its double layer under various load conditions and evaluates the stiffness of the boundary rings. It demonstrated that the largest deformation δ occurs in LC4, wind from the back, with 10 mm in the flat back area with the outer ring ovalizing by 4 mm (Fig. 13a). The active-bending stresses had no impact on the results. LC1, concrete load, would result in 6.8 mm deformation in the top area with no ring ovalization (Fig. 13b). Hence, the gridshell performed better under the concrete load corresponding to the funicular distribution than the wind.

This stands in accordance with its axial force transfer (Fig. 13c) that

Fig. 10. Results from FE form finding of the bending-active gridshell with deviations Δ to the funicular target (left) and deformations δ between the steps (right) in mm with A for amplitude: (I) formation phase by (a) insertion of separate splines, (b) connection at spline crossings, (c) connection to the second layer with distancing stirrups, (II) locking phase by (d) connection of bracing stirrups, and finally (III) boundary adjustment phase by (e) removal of the inner ring props.

Fig. 12. Load cases of (a) concrete ribs LC1; (b) CFD result interpreted to (c) wind from front LC3; (d) wind from back LC4; (e) wind from side LC5; values to be multiplied by the tributary areas.

matches the funicular one (Section 3.1), even with inner props. In the wind load cases, the ribs are also activated in bending, activating the static height with one spline in tension and one in compression (Fig. 13d). Thus, the bending acts on two levels – the ribs and the splines themselves. The spline bending (Fig. 13e), generated by the stirrups that activate the rib bending, is 1/10 smaller than the active bending moments (Section 3.2). The even smaller bending in the rings justifies that these are designed similarly to the ribs (Section 2.2).

The structure's stability is safe by a minimum buckling load factor χ of 2.7 in the concrete load case. It occurs in the flattest area at the back in the most compressed and longest spline segments (Fig. 13f). Again, the active bending stresses do not influence the result noteworthily.

The maximum connection forces within the gridshell's ribs arise in the connection of the spline crossings and to the bracing stirrups with 0.95 kN in the areas subject to the highest deformation with wind from the back (Fig. 13g). Physical experiments proved that the metal wire tie connections can withstand these.

*4.3. Sensitivity to the stirrup types and density*

The falsework's structural sensitivity to the activation of the double layer by the stirrup types and their density is demonstrated by its displacement δ and stability as buckling load factor χ under full wet-concrete load, LC1 with inner props. Fig. 14 shows the numerical investigation results from models with no stirrups at all, only distancing, only bracing, a lower density of distancing and bracing, an informed mix of the lower and full density of distancing and bracing, and a full density of distancing and bracing stirrups. The informed mix is chosen such that 30% of the ribs, in the area critical to buckling and higher deformations at the back and top, are equipped with the full density while the remaining ribs with the lower density. No further segment-wise differentiation was performed to keep construction logistics simple.

The falsework without any stirrups suffers stability failure under the wet-concrete load. The distancing stirrups allow the structure to reach a stable state under the wet-concrete load, however, with large deformations and without sufficient stability safety. With bracing stirrups
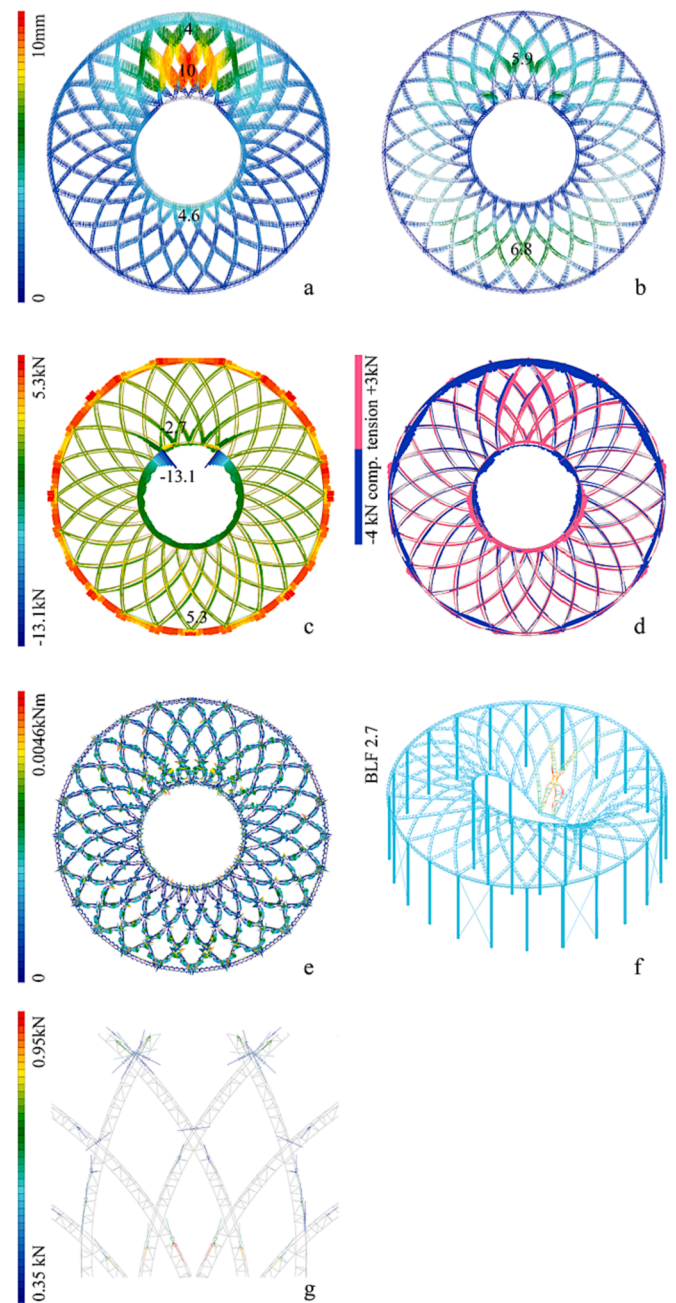
Fig. 13. Structural analysis results: (a) deformation δ from dominant wind load case from the back versus (b) from the funicular full concrete load; (c) axial forces in the funicular concrete load case; (d) axial forces in the wind from the back; (e) bending moments without active bending in the funicular concrete load case; (f) buckling failure at a load factor χ of 2.7 for full concrete load; (g) connection forces in the wind from back load case (only displayed if above 0.35 kN).

instead of distancing stirrups, the displacements δ halve and the buckling load factor χ doubles. This highlights the bracing stirrups' critical role in the gridshell's structural performance. However, the distancing stirrups are essential for shape control (Section 3.2) and to prevent rotation of the spacers. The results improve significantly if both stirrup types are combined with full density. Half the density for both stirrup types results in worse performance than with bracing stirrups only. However, the mixed density performs nearly as well as the full density while its stirrup mass is reduced by nearly 30%.
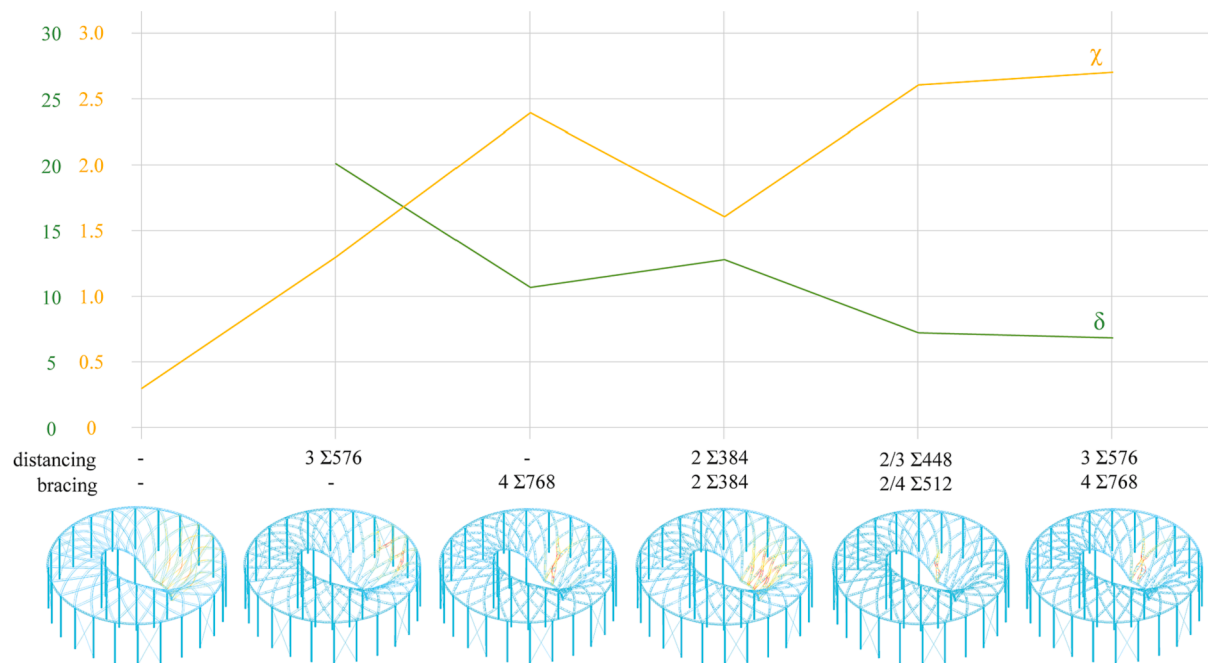
Fig. 14. Numerical investigation on the influence of the stirrup type (distancing or bracing) and density (indicated per rib segment and in total) on the displacements δ [mm] and stability χ (buckling load factor) of the gridshell under wet-concrete load.

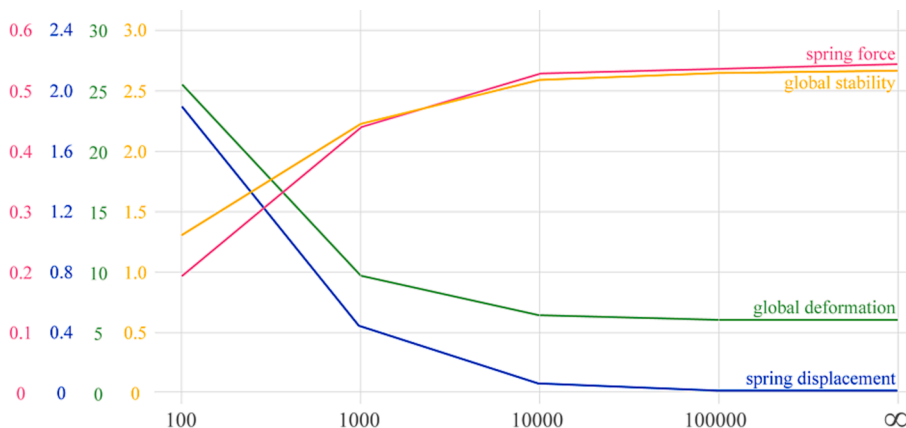### 4.4. Sensitivity of the connection stiffness

The relevance of the internal connection design on the gridshell's structural integrity is demonstrated with a sensitivity study with varying connection stiffnesses of the crossings of the splines and of the splines to the stirrups (as introduced in Fig. 9). The spring stiffness **c** was varied on a logarithmic scale from 100 kN/m to 100,000 kN/m and compared with infinite stiff, rigid node couplings (x-axis). The investigation evaluates the force and displacement in the spring connections and their effects on the structure's global deformations **δ** and stability (y-axis). The analysis was performed for LC1.

The spring force **f** and displacement **Δ** have the linear relation of **f** = **c** **Δ**. The results in Fig. 15 show that the spring force **f** and global stability of the buckling load factor **χ** increase proportionally as the spring displacement **Δ** and global deformations **δ** decrease proportionally. The graphs reveal that there is no significant improvement after a stiffness **c** of 1000 kN/m. The connection stiffness **c** of 1000 kN/m is a realistic assumption for the wire tie connections, as 1 kN would cause a deformation of 1 mm. It results in sufficient structural integrity and is taken further for subsequent investigations. Moreover, this investigation highlights the sensitivity of the global shape on the target crossing alignment.

4.5. Sensitivity of the casting sequence

To demonstrate the suitability of the gridshell as falsework, its geometric integrity must be structurally investigated for a stepwise casting sequence. The concrete must be cast stepwise into the rib's closed moulds to limit its hydrostatic pressure onto the textile shuttering and spacers. Physical experiments demonstrated that these could withstand over 1.5 m concrete height [18]. This research's scope excludes the discourse on the resulting cold joints. The study in Fig. 16 investigates the geometric impact and structural performance of the gridshell false-work under a stepwise casting sequence. The model incorporates the connection stiffness **c** of 1000 kN/m from Section 4.4 and is temporarily propped along the inner ring.

The wet-concrete load is applied in intervals roughly from one dia-grid crossing to another against the gravity direction. In each subsequent load case, the stresses and deformations of the primary load case are added, and the stiffness of the previously loaded interval is increased by a factor of 10 as it will be hardened and locked in its previously deformed shape by then. Essentially this results in a pairwise propagation of a stiffened and loaded area for the semi-hardened concrete area, a loaded but not yet stiffened area for the freshly concreted area, and an

Fig. 15. Numerical investigation on the influence of the connection stiffness (introduced in Fig. 9) (x-axis) on the structural performance of the gridshell. Connection spring stiffness [kN/m] in logarithmic scale to spring connection force [kN] (pink), spring connection displacement [mm] (blue), global coordinate deformation δ [mm] (green), and global stability as buckling load factor χ [-] (yellow). (For interpretation of the references to colour in this figure legend, the reader is referred to the web version of this article.)
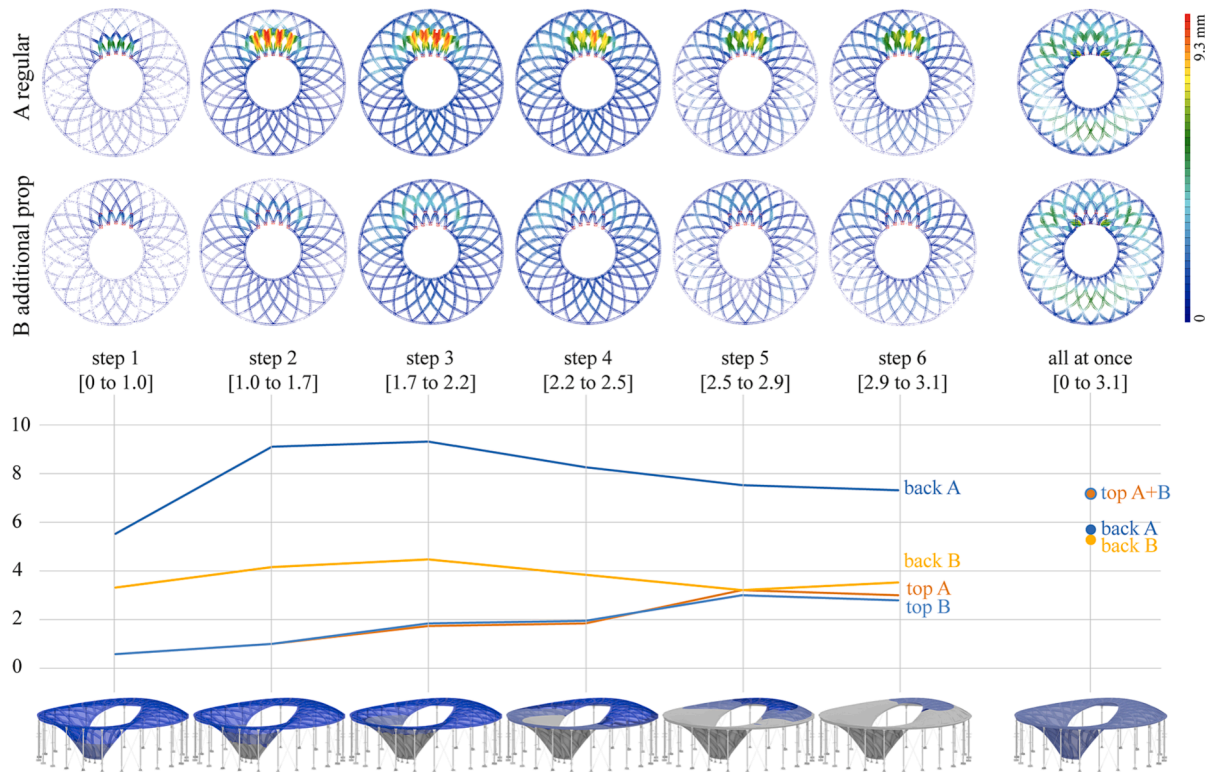
Fig. 16. Numerical investigation on the influence of the potential casting strategy on the displacement δ [mm] of the gridshell under concrete load for the regular and additionally propped gridshell.

unloaded area. The stiffening is crucial; otherwise, the structure would behave as if it was loaded at once. Geometric nonlinear analysis in third-order theory ensures finding equilibrium in each deformed state.

High displacements **δ** occur in the back area of low geometric stiffness and long segment length between diagrid crossings. If the gridshell was additionally propped at these crossings, the displacements would reduce by half (Fig. 16, compare A to B). However, especially in the model without additional props, subsequent load steps decrease deformations as they rebalance by pushing the rigidified elements back upwards. Higher stiffness values for the already hardened intervals lead to lower deformations in the second step but also less compensation in subsequent steps. Hence, a longer curing time would not improve results significantly. The largest displacement increase occurs in steps 1 and 2; consequently, these could be divided into smaller intervals to reduce displacements. In general, the intervals were not optimised to represent a realistic construction scenario. Other measures could double up the splines in the critical area or generally avoid low double curvature as a global design constraint. However, the deformations in the back without additional props are just as large as to cancel out the deformations that occurred during form finding of the gridshell.

The top area is not affected by the props; both models perform almost the same, with a deformation increase towards the last intervals with a lower magnitude compared to the back. If the concrete were cast at once without incremental hardening (Fig. 16, right), the deformations would be more distributed because the areas rebalance each other freely; the top deformations would be significantly higher, and the back deformations would lie in between. The additional props would hardly have an effect.

5. Fabrication

5.1. Construction sequence

The construction process of the KnitNervi divided itself into a pre-fabrication phase (Section 5.2) and an in-situ construction phase

(Section 5.3). The prefabrication provided a kit-of-parts of reinforcement steel splines, stirrups and boundary rings (Fig. 17a), which was compact and lightweight for transportation onto the site. The on-site construction commenced with the installation of the steel scaffolding props (Fig. 17b). Then the gridshell ring segments, prefabricated as rebar cage segments, were manually lifted in, adjusted in height by the telescopic props and connected (Fig. 17c). The perimeter bracings were installed and pretensioned.

The installation of the gridshell ribs relied on an incremental process of simple assembly steps that gradually transformed the kit-of-parts into the load-bearing rebar cage. The bending-active form-finding simulation in Section 3.2 directly informed this sequence, and the construction serves for its validation.

In between the two rings, the lower direction of the upper layer of spline pairs was actively bent in and anchored to the rings (Fig. 17d), followed by the upper direction of the upper layer (Fig. 17e). The subsequent process ensures that the splines are not interweaved. The sequence avoids collision of the to-be-bent upper layer with the installed layer. The stirrups were loosely slid on prior to the second end-connection to avoid tedious attachment later. The resulting diagrid was connected precisely at target crossing marks leading to the tremendous refinement and stiffness increase (Fig. 17f).

Subsequently, the lower diagrid layer was inserted by sliding the splines through the stirrups commencing with the lower direction (Fig. 17g) and subsequently with the upper direction (Fig. 17h). Also, the lower splines were connected at their target crossing marks (Fig. 17i). The placement of the distancing stirrups constrained the layers into constant spacing, refining the geometry slightly. Then the bracing stirrup pairs locked the gridshell's shape and activated the full structural depth resulting in the completed triangular rebar cage (Fig. 17j).

The double-layered falsework was then encased by the knit shuttering by clipping on the plastic spacers and then clipping in the metal shaping rods inserted into the knit sleeves to mount the knit strips (Fig. 17k). As stated in Sections 1.3 and 1.5, the design, fabrication, sequence, and installation of the knit are not subject to this publication.
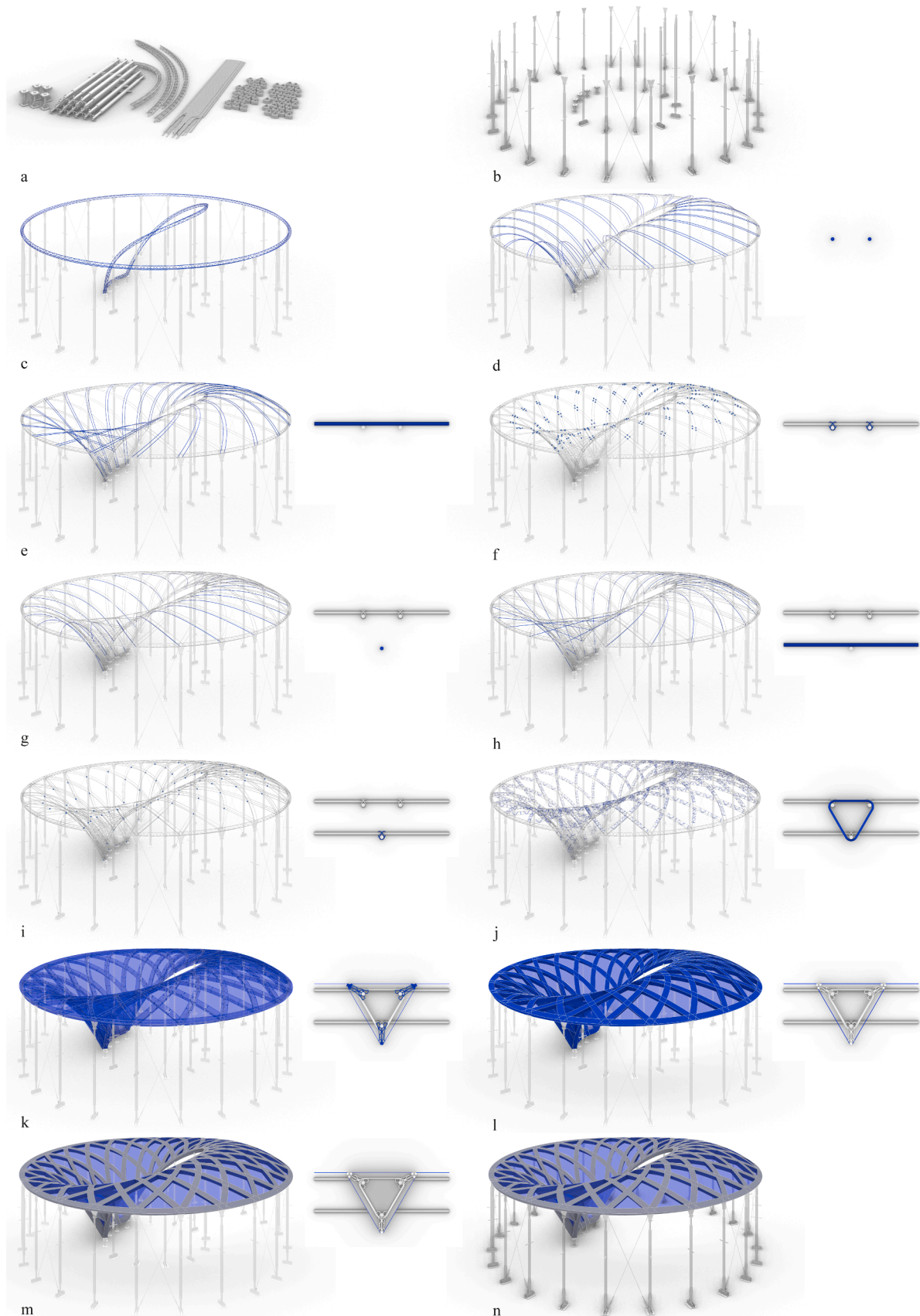
Fig. 17. Sequence of the construction steps comprising (a) kit-of-parts, (b) reusable steel props, (c) rebar gridshell boundary rings, (d) lower direction of upper layer rebar splines, (e) upper direction of upper layer rebar splines, (f) crossing connection of upper splines at marked positions, (g) lower direction of lower rebar splines, (h) upper direction of lower rebar splines, (i) crossing connections of lower splines at marked positions, (j) stirrup and inclined stirrup placement, (k) knit shuttering installation with spacers and rods, (l) potential knit impregnation, (m) potential concrete casting, and (n) removal of the temporary props of the inner ring.

Then, in principle, the knit could be impregnated with epoxy resin (Fig. 17l), and the concrete ribs could be cast in the stepwise sequence (Section 4.5) (Fig. 17m). As a final step, the temporary scaffolding props of the inner ring were removed (Fig. 17n).

5.2. Prefabrication of the kit-of-part of the gridshell

The prefabrication validated whether the preparation of the kit-of-parts of the gridshell was feasible pragmatically and with reasonable logistics. All the measurements for the rebar positions were retrieved from the COMPAS assembly graph data structure. Axis-symmetric splines in the opposite direction differed in total and segment length to account for the collision-free crossing by its 10 mm offset. Each spline was identified by a unique key and attributes for its respective position, layer affiliation and mounting sequence.

The rebar splines were cut to measure with an angle grinder, marked at the target crossings and threaded at their ends with a cutting die (Fig. 18a). These simple repetitive tasks were conducted by untrained
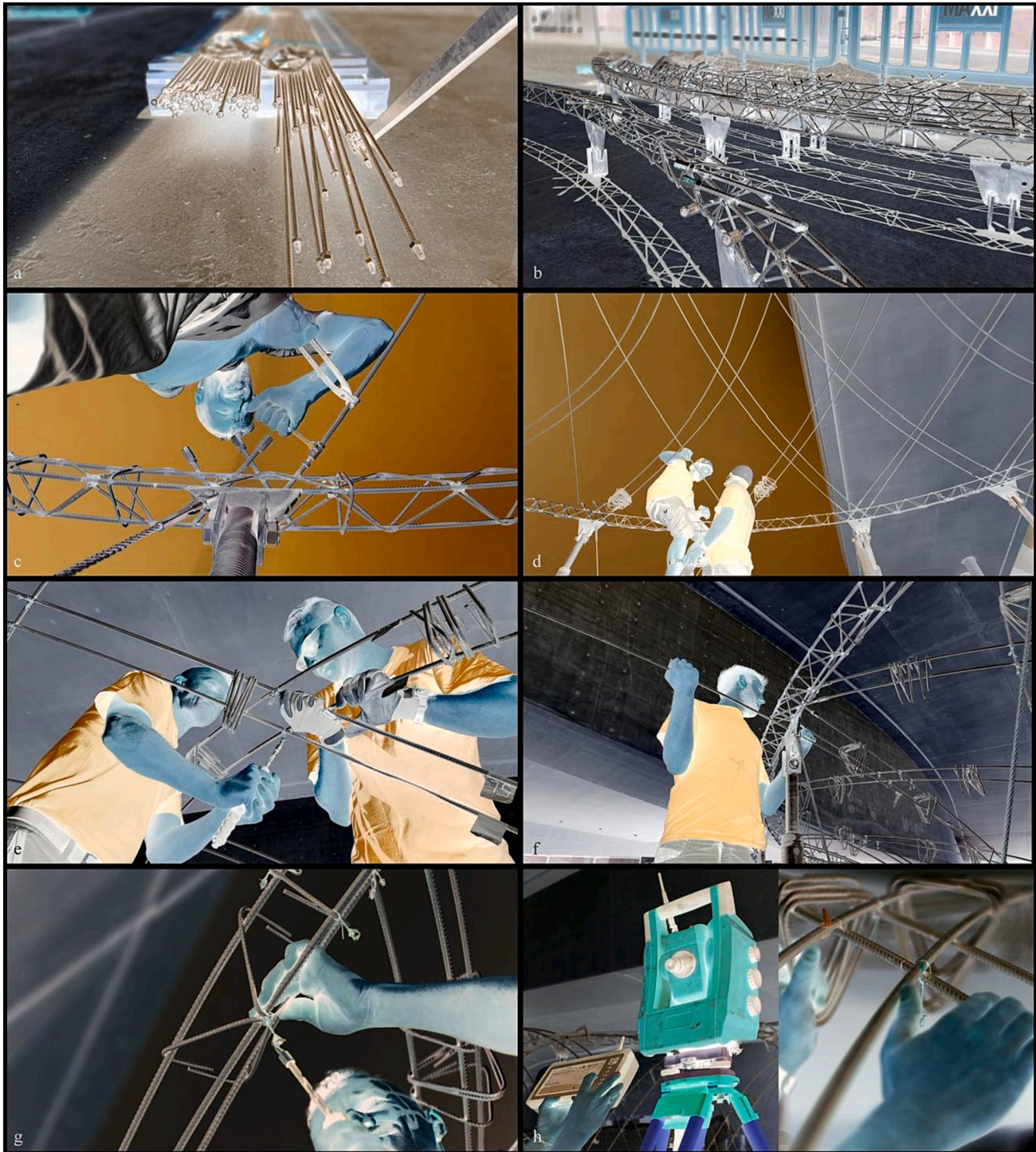
Fig. 18. Construction of KnitNervi with (a) prefabricated rebar splines with threaded ends, (b) prefabricated rebar truss rings segments, (c) threaded connection of spline to rings, (d) active bending of rebar splines, (e) spline crossing connection with wire ties, (f) insertion of lower spline layer, (g) positioning with wire ties of bracing stirrups, and (h) EDM-measurement at crossings with a total station (photo: (g) and (h) by Thom de Bie).

labour but could be automatised depending on the context. The triangular stirrups were plastically formed by an industrial rebar manufacturer in a rebar bending machine. Their bending radius is limited, leading to imprecise corners; therefore, larger scales or smaller cross-sections would improve precision. For the prefabrication of the rings (Fig. 18b), the splines were guided through jig plates to restrain them into the target shape and then welded with the spline connectors and bracings to lock the bending. Their spline ends were also threaded to connect the segments.

5.3. On-site construction of the gridshell

The on-site construction validated whether the assembly process was feasible pragmatically and with reasonable logistics. On-site in the MAXXI's courtyard, the scaffolding props were easy to mount by a single worker, and the rings were sufficiently lightweight to be lifted in without the need for a crane. A single spline's active bending and connection required one pair of construction workers (Fig. 18d). In the highly curved splines with higher actuation force, a third worker assisted the positioning at the end connection. The threaded end connection requires axis alignment and must avoid a gap, as the threads on both sides are unidirectional. The connector nut was pre-mounted on one side, positioned over the joint and fixed with a pair of wrenches (Fig. 18c). The alignment of the splines' target crossings required forceful manipulation (Fig. 18e). The highly curved splines were challenging to constrain. As the shape outcome is highly sensitive to the precise spline and segment length, gaps or crossing misalignments became obvious and could mostly be corrected. The connections were executed firmly with the wire tie tool to achieve high connection stiffness for structural integrity (Section 4.4).

The curvature of the lower spline layer was well guided by the stirrups hanging from the upper layer (Fig. 18f). The ring did not provide connector splines for these yet; hence these were welded on-site. In principle, the threaded connectors would have been aligned with ease as the direction was already enforced. The connection of the stirrups was carried out with the wire tie tool by single workers (Fig. 18g).

All tasks were typical for the low-tech rebar worker industry and could be conducted on ladders and movable platforms. The construction crew was composed of one worker trained for welding and with construction expertise and three untrained workers.

5.4. Geometric measurement and calibration with a total station

The structure was surveyed throughout the construction process with a total station employing Reflectorless Electronic Distance Measurer (EDM) (Fig. 18h). The measurements served to calibrate the ring positions, then to track the gridshell's shape evolution towards its target and validate the form-finding simulation, and finally, to evaluate the precision of the completed gridshell.

6. Results

KnitNervi's geometric and structural design and construction resulted in a load-bearing rebar cage that could serve as shape-defining falsework and integrated reinforcement for a ribbed concrete shell (Fig. 19a). It was wrapped with a textile knitted shuttering which was of vibrant blue colour and set a highlight in the MAXXI museum's courtyard (Fig. 19b). The resulting triangular cross-sections are crisp and reveal the construction system like an X-ray (Fig. 19c). By structural design choice, the props cannot be removed. However, the design suggests that the structure could span beyond, for example, merge with other funnels and thus self-stabilise, as in explorations by Rippmann and Block [5].
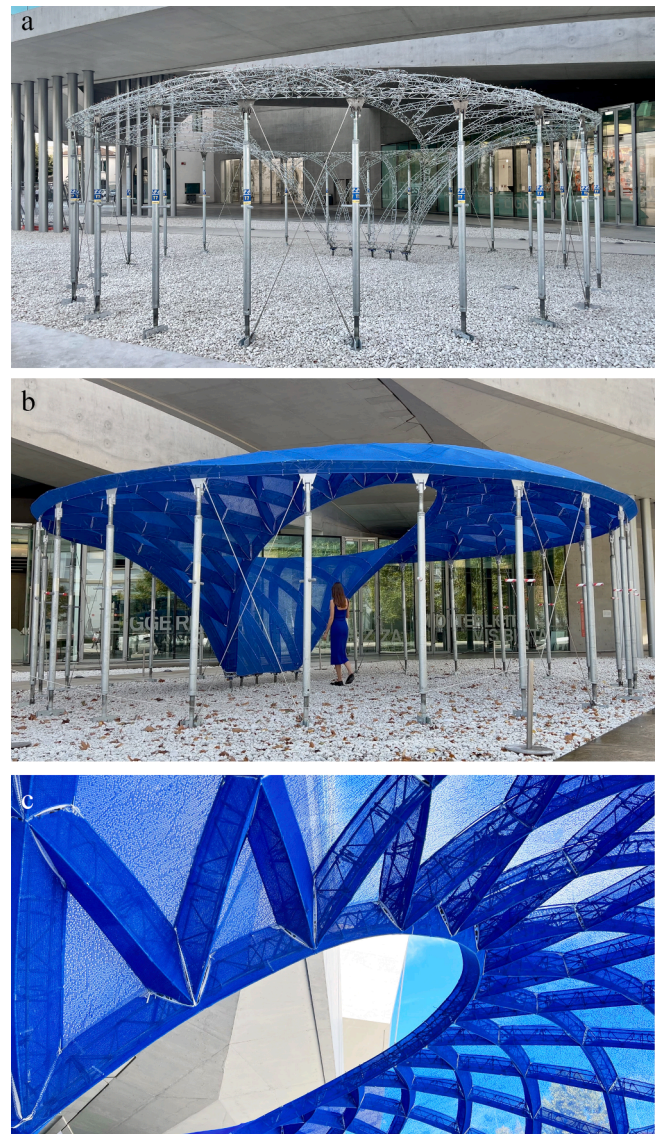

Fig. 19. KnitNervi demonstrator at MAXXI, Rome (a) at the stage of the completed double-layered gridshell structure that serves as falsework and reinforcement, (b) with the knitted shuttering from an external perspective and (c) as an internal closeup with oculus and prismatic sections with rebar cages inside.

6.1. Geometric precision

The assembly process of the gridshell was in agreement with the simulations in Section 3.2. The main shape change from the bending-active Elastica shape of the gridshell towards the funicular target shell occurred when connecting the diagrid crossings; a minor shape refinement was assessed when connecting the second layer with the distancing stirrups; and the release of the props of the inner ring did not result in a significant shape change.

Fig. 20 shows the deviations **Δ** of the materialised gridshell demonstrator in its completed state to the ideal funicular target geometry. The results are generated from EDM coordinates measured at intersections of the upper spline layer and the ring (Section 5.4). Few intersections could not be surveyed as the gridshell obstructed them.

Table 1 reveals with the arithmetic average and absolute deviations **Δ** per part that the accuracy at the outer ring is much higher than at the inner ring of more complex geometry. These inaccuracies in the boundary conditions propagate with amplification to the gridshell ribs.
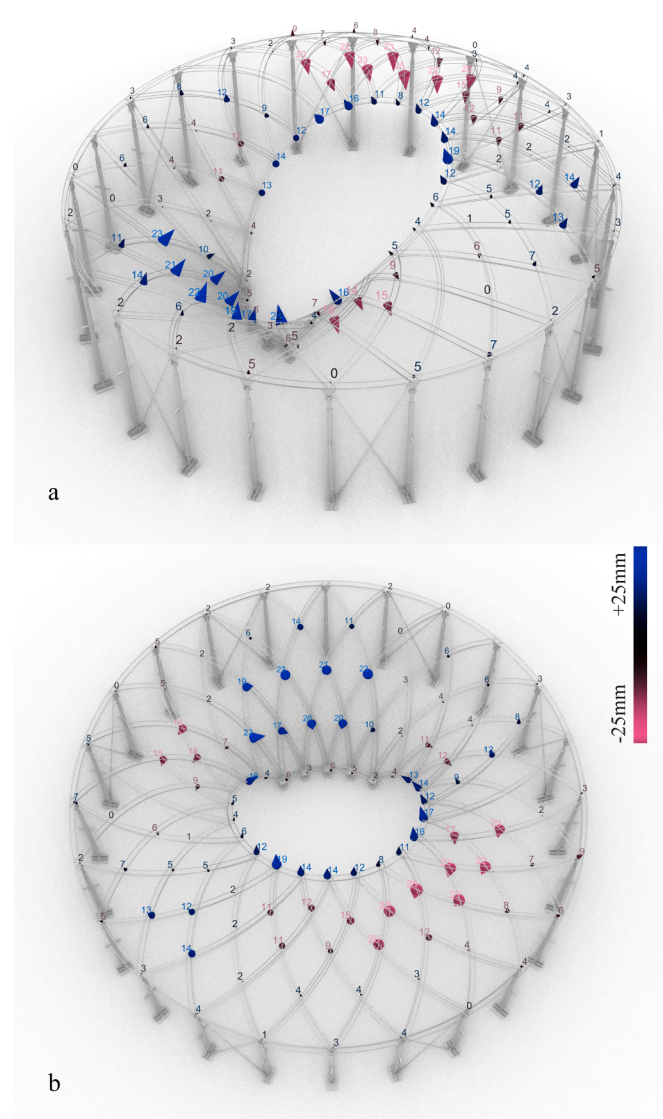
Fig. 20. Deviations Δ of the physical gridshell demonstrator to the ideal funicular target geometry shown with a (a) side perspective and (b) top perspective in mm with a gradient from pink for downwards to blue for upwards deviations.

Table 1
Deviations Δ of the physical gridshell demonstrator to the ideal funicular target geometry per part in mm.

Part	Arithmetic average	Absolute maximum
Ribs	3.8 mm	25 mm
Outer ring	10.2 mm	9 mm
Inner ring	11.1 mm	19 mm
Overall	**9.5 mm**	**25 mm**

The symmetric perspective in Fig. 20b indicates that the deviations are not axis-symmetric as the structure is. Accuracy is worse on the right side of the top area where the ribs connect to the inner ring's least-accurate section and on the left side in the back area close to the ground supports where the kink in the inner ring was off. These were also the areas where the alignment of the spline crossings to the marked positions was challenging. This highlights the importance of segment lengths in defining the global geometry. Simultaneously, this shows that these large deviations are not inherent to the construction design and could be avoided by more precise boundaries and enforcing the spline crossing targets.

Besides these errors, the deformation mode stands in good agreement with the gridshell's bending-active form-finding simulation, where the back also deforms upwards, the top downwards and the inner ring slightly upwards (Fig. 10e*).

6.2. Structural mass

Table 2 lists the positions used in the gridshell and scaffolding of the KnitNervi demonstrator with their respective type, quantity, and mass. The structure's total weight sums up to 1.3 tons, with 0.6 tons from the gridshell falsework and 0.7 tons from the scaffolding. The falsework's weight per shell surface area is $9.2 \, kg/m^2$. This number excludes the scaffolding, as these are reusable or removed in the design outlook.

Within the gridshell, the splines constitute the greatest mass share, with 67%. Reducing their cross-sections to 8 mm would reduce their weight by 144 kg. The design could change to higher bending curvatures; however, the slenderer cross-section could cause stability problems (Section 4.2). In contrast, if 4 mm diameter rebar were commonly available for the stirrups and bracings, it would facilitate manufacturing and accuracy without affecting structural performance. This would save 89 kg with an impact of 15% on the gridshell's total weight.

6.3. Construction time

The on-site construction of the scaffolding and gridshell required a total net time of 36 h with a construction crew of 4 workers. This timekeeping excludes downtime due to problem-solving, delivery delays, and measurements. Table 3 subdivides the tasks in correlation to the construction steps in Fig. 17.

The construction time divides itself into one day on the scaffolding

Table 2
Material, quantity and weight of the positions for the gridshell falsework and scaffolding.

	Component	Type	Mass per unit	Quantity	Total Mass
Gridshell	Splines	PreZinc rebar 10 mm	0.617 kg/m	646 m	399 kg
	Distance stirrups	PreZinc rebar 6 mm of length 0.4 m	0.09 kg	458	41 kg
	Bracing stirrups	PreZinc rebar 6 mm of length 0.46 m	0.10 kg	776	78 kg
	Ring bracings	PreZinc rebar 6 mm	0.222 kg/m	200 m	44 kg
	Connecting nuts	Zinc plated M10x30mm BN1933	41 g	348	14 kg
	Nuts	Zinc plated M10x8mm BN117	10 g	696	7 kg
	Tie wires	Loop wires, doubled as cross tie	4 g	3674	15 kg
					598 kg
Scaffolding	Props	Doka spindle strut T7	26.2 kg	24	626 kg
	Ring supports	Custom welded steel plates	2.4 kg	24	58 kg
	Bracings	Jakob wire rope 8 mm with clevis and turnbuckle	1.4 kg	16	22 kg
					706 kg
					1304 kg

Table 3
Construction time with a construction crew of four workers.

Part	Component	in Fig. 17	Duration
Scaffolding	Foundations		7 h
	Props	b	1 h
	Bracings		1 h
			9 h
Gridshell	Rings	c	3.5 h
	Splines in 1st direction of upper layer	d	3.5 h
	Splines in 2nd direction of upper layer	e	3.5 h
	Wire tie connections of upper layer	f	2 h
	Splines in 1st direction of lower layer	g	1.5 h
	Splines in 2nd direction of lower layer	h	1.5 h
	Wire tie connections of lower layer	i	1 h
	Stirrups	j	10 h
	Temporary scaffolding removal	n	0.5 h
			27 h
			36 h

and three days on the gridshell. For the scaffold, the longest time was spent on the foundation work, which is highly dependent on the sub-structure condition, while the industry-optimised scaffolding props were erected within 1 h. Within the gridshell, the installation of the upper layer took twice as long as the lower layer. Even though there are twice as many splines in the upper layer, the main reason was the tedious alignment of the threaded connection for the highly curved splines (Section 5.3). The stirrup tying that demanded 37% of the gridshell's construction time could be executed simultaneously such that more untrained workers would have sped up the process linearly.

7. Discussion

This research introduced a construction system for forming and reinforcing a funicular concrete skeleton shell with a diagrid of complexly-curved ribs. The integrated formwork system was demonstrated at an architectural scale with the realisation of the expressive KnitNervi pavilion. It resulted from the co-design methods of the interrelated design, engineering, and construction of the integrated formwork for the reinforced concrete structure. This process was enabled by its implementation within one comprehensive computational framework, COMPAS.

The system design (Section 2) met the research objective to design and detail a falsework structure that can simultaneously serve as integrated reinforcement with sufficient concrete coverage and provide a spatial substructure that supports a closed-mould shuttering for shaping skeleton ribs. This was demonstrated with the nodal prototypes (Fig. 2).

The geometric design (Section 3) met the research objective to control the shape of the bending-active gridshell falsework towards the funicular target, composed of syn- and anticlastic curvature, with a maximum deviation of 8.5 mm. The 3D geometry was defined by the lengths and crossing positions of the splines, and the distancing stirrups refined the shape, while the shear-connecting stirrups activated the double-layered sections for stiffening.

The structural design (Section 4) met the research objective to engineer and detail the gridshell such that it performs as falsework with sufficient load-bearing capacity and serviceability to support the weight of the wet concrete at an architectural scale. The boundary rings could sufficiently restrain the gridshell, the double layer was successfully activated by the stirrups, and the combination of the stirrup types and density was a compromise in terms of mass and structural performance. Moreover, the detailing of the internal connection revealed the sensitivity of the global shape on the stiffness and crossing positions. Most importantly, if the gridshell were additionally propped at the critical crossings in the lower back of the structure, the maximum deformations would lie below 4 mm for the stepwise casting sequence.

The fabrication (Section 5) met the research objective to realise the gridshell efficiently and pragmatically such that the system design,

shape control, and stiffening strategies satisfy expectations on adequate precision, logistics, time, and material resources. Through the decision taken on the assembly sequence, the research demonstrated congruence between the form-finding simulation and the demonstrator's on-site assembly. Standard straight rebars were rapidly assembled into a complex bespoke shape with fabrication, including detailing designed such that it required only a pair of construction workers with low-tech conventional tools for rebar tying. The resulting rebar cage, however, combines the two functions of an integrated reinforcement with a load-bearing falsework, which supports the novel cross-sectional flexible formwork.

7.1. Advantages

The complex structural geometry provides the efficiency to the funicular concrete skeleton shell. However, it would be complex to form and reinforce when using rigid moulds and conventional reinforcement solutions. Instead, the presented system foregoes the need for expensive, high-tech, custom, prefabricated moulds, which would be volumetrically inefficient for transport, result in waste as single-use products, and require dense substructures; it also foregoes the need for expensive, custom prefabricated, pre-bent rebar cages, which would be inefficient for transport and tedious in assembly. Instead, the self-supporting, stay-in-place, integrated falsework synergises both efforts of labour, material, and cost for the process and structure with minimal material, low-tech prefabrication, compact transport, and low-tech assembly of light-weight elements without the need for costly cranes, substructure, waste, and extra demoulding steps.

In comparison to the state-of-the-art tensile flexible formwork systems, it also enables synclastic shapes and integrates the boundary beams into the system with the same materialisation language and function. It scaled up the bending-active flexible formworks through its shear-connected double layer. And it resolves the reinforcement question. Compared to the integrated reinforcement references, the degree and density of reinforcement are lower because of the structurally-informed shape. Furthermore, its pragmatic fabrication does not limit its application to digital fabrication contexts, as the bending-active logic determines the shape. In comparison to the flexible formworks and integrated reinforcement references, innovation lies in the skeleton rib articulation instead of continuous shell surfaces.

7.2. Potential improvements and general limitations

Technical improvements could be achieved by putting bounds on the curvature range of the shell: a lower limit to avoid reduced geometric stiffness in flatter parts and an upper limit to avoid geometric deviations caused by misalignment of the prescribed crossings of the splines with high bending resistance. Furthermore, more precise boundaries would improve global precision. Complexity and time could be reduced by facilitating the alignment of the end connectors by a slight modification of their detailing.

It was beyond the scope of this research to implement computational methods for an informed precamber to approximate the funicular target shape with higher precision under the concrete load through numerical optimisation [37] and active control [38]. In addition, on-site shape control could be refined by prescribing and enforcing the relative position of the shear-connecting stirrups, for example, at the crossings or by a third grid direction, for example, with tensioning cables that distort the diagrid cells in the contracting direction for Gaussian curvature [39]. Further research could investigate the on-site deployment of a partially pre-assembled gridshell to speed up and simplify the on-site construction time and logistics. Replacing one of the two bending-active layers with tensile elements could lead to a more self-contained and light-weight system but would possibly make its equilibrium more sensitive.

7.3. Future work

To widen the applicability of the proposed system, future work will investigate its scalability and suitability to other designs and architectural typologies such as bridges, wildlife crossings, vaulted floors, and funicular roofs, including those with funnel columns [5] or the new Stuttgart main station [34]. The workflow is reproducible through the open-source framework COMPAS, and the design is geometrically configurable to various bespoke designs. The fabrication is, in principle, unlimited in terms of rebar lengths; however, the actuation force might exceed human capacities. However, primarily the scalability of the gridshell is limited due to the nonlinear upscaling of the bending-active behaviour. A sensitivity study will evaluate the maximum possible size up to which the system can be actively bent and structurally perform as falsework and which measures could circumvent the limitations.

The shuttering could increase its functionality by integrating textile reinforcement [40] or, depending on the context, could be simplified to off-the-shelf industrial fabrics that would entail sewing prefabrication but would not be limited to high-tech construction contexts.

A research study must be conducted to quantify the environmental benefits of this type of construction system in comparison to other formwork and reinforcement approaches and to a conventional structure with non-structural geometry. Furthermore, this study could suggest measures to improve sustainability further. An alternative system design could focus on an unreinforced funicular concrete structure with external, non-integrated falsework allowing for a clean separation of parts at the end of its lifecycle. The falsework could be designed for disassembly and reuse, materialised with more sustainable choices depending on its robustness requirements. The spacers and shuttering rods would become obsolete as the falsework would directly tauten the flexible shuttering. The system of reduced complexity would, however, be applicable only to strict funicular shapes.

8. Conclusion

This paper presented a combined formwork and reinforcement system for efficiently constructing concrete structures of bespoke double-curved geometry with unique ribbed articulations. Its system design, structural performance, and construction process, with all their interdependencies, were demonstrated at an architectural scale in the proof-of-concept demonstrator KnitNervi.

The concept relied on a bending-active gridshell materialised as a rebar cage that simultaneously served as both falsework and reinforcement. Its shear-connected double layer of splines provided shape control for a lightweight, load-bearing falsework. Its materialisation as a rebar cage employed standard rebar materials and low-tech manufacturing techniques, allowing compact transport and short construction time. These basic construction principles combined with the geometric, structural, and assembly logic proved to be an extremely efficient construction method for complex geometry, which would have been complex to build with conventional formwork and reinforcement approaches.

Structural geometry provides the basis for the efficiency of both the flexible formwork system and the resulting concrete skeleton shell. The system offers a customisation strategy independently of digital fabrication, allowing the construction of highly material-efficient structures of reduced embodied carbon without the need for wasteful moulds. When applicable to a variety of spanning structures at architectural scales in a range of technological construction contexts, this research could open up opportunities to improve the sustainability of such.

Declaration of Competing Interest

The authors declare that they have no known competing financial interests or personal relationships that could have appeared to influence the work reported in this paper.

Comments

All images, unless stated otherwise, and the text are by the first author.

Appendix

The following making-of video provides a visual summary of the design and construction of the project: https://vimeo.com/764092499.

Full credits KnitNervi project

Design:

ETHZ BRG: Lotte Scheder-Bieschin, Serban Bodea, Tom Van Mele, Philippe Block; TUDelft: Mariana Popescu, Nikoletta Christidi

Structural engineering:

ETHZ BRG: Lotte Scheder-Bieschin, Philippe Block

Knitted formwork:

TUDelft: Mariana Popescu, Nikoletta Christidi

Fabrication and construction:

ETHZ BRG, gridshell: Kerstin Spiekermann, Lotte Scheder-Bieschin, Serban Bodea, with support of Eva Schnewly, Damaris Eschbach, Rolf Imseng, Stefan Liniger; TUDelft, knit: Mariana Popescu, Nikoletta Christidi

Project and site construction coordination:

ETHZ BRG: Serban Bodea; TUDelft: Mariana Popescu

Exhibition content, coordination, and curation:

Lotte Scheder-Bieschin, Serban Bodea, Mariana Popescu, Kerstin Spiekermann, Noelle Paulson, Katharina Haake, Philippe Block with support of Eva Schnewly, Rolf Imseng

Sponsors:

NCCR Digital Fabrication, ETH Zurich, Debrunner Acifer Bewehrungen, Doka Switzerland and Italy, Jakob Rope Systems, NOWN, Symme3D, Gisler Bewehrungen AG, Berner Fachhochschule

Documentation and Video:

Footage: Thom de Bie, Mariana Popescu, Lotte Scheder-Bieschin, Serban Bodea; Editing: Thom de Bie; Animations: Lotte Scheder-Bieschin, Michele Capelli, Gabriele Mattei

References

[1] UN Environment Programme. 2022 global status report for buildings and construction: Towards a zero-emission. Nairobi, Kenya: Efficient and Resilient Buildings and Construction Sector; 2022.

[2] Lehne J, Preston F. Making concrete change; innovation in low-carbon cement and concrete. London, UK: Energy Environment and Resources Department; 2018.

[3] De Wolf C, Ramage M, Ochsendorf J. Low carbon vaulted masonry structures. J Int Assoc Shell Spatial Struct 2016;57(4):275–84.

[4] Block P, Van Mele T, Rippmann M, Ranaudo F, Calvo Barentin C, Paulson N. Redefining structural art: Strategies, necessities and opportunities. Struct Eng 2020;98(1):66–72.

[5] Rippmann M, Block P. Funicular funnel shells. In: Gengnagel C, Kilian A, Nembrini J, Scheurer F, editors. Proceedings of the design modelling symposium Berlin 2013: Rethinking Prototyping, Berlin, Germany: 2013, p. 75–89.

[6] De Wolf C. Low carbon pathways for structural design: embodied life cycle impacts of building structures. Thesis. Massachusetts Institute of Technology; 2017.

[7] Adriaenssens S, Block P, Veenendaal D, Williams C, editors. Shell structures for architecture: form finding and optimization. Abingdon & New York: Routledge Taylor & Francis Group; 2014. 10.4324/9781315849270.

[8] Kudless A, Zabel J, Naeve C, Florian T. The design and fabrication of confluence park. In: Burry J, Sabin J, Sheil B, Skavara M, editors. Fabricate 2020. London, UK: UCL Press; 2020. p. 28–35.

[9] Peri Group. Freeform Formwork 2020. https://www.peri.ltd.uk/products/formwork/special-formwork/freeform-formwork.html (accessed December 14, 2022).

[10] Jipa A, Dillenburger B. 3D printed formwork for concrete: state-of-the-art, opportunities, challenges, and applications. 3D Print Addit Manuf 2022;9(2):84–107.

[11] Méndez Echenagucia T, Pigram D, Liew A, Van Mele T, Block P. A cable-net and fabric formwork system for the construction of concrete shells: design, fabrication and construction of a full scale prototype. Structures 2019;18:72–82. https://doi.org/10.1016/j.istruc.2018.10.004.

[12] Block P. Thrust network analysis: exploring three-dimensional equilibrium. Massachusetts Institute of Technology; 2009.

[13] Van Mele T, Lachauer L, Rippmann M, Block P. Geometry-based understanding of structures. J Int Assoc Shell Spatial Struct 2012;53:285–95.

[14] Van Mele T, Casas G, Rust R, Lytle B, Chen L. COMPAS: A computational framework for collaboration and research in Architecture, Engineering, Fabrication, and Construction. 2022.

[15] Van Mele T. compas_tna: Implementation of the Thrust Network Analysis based on COMPAS 2022.

[16] Popescu M, Rippmann M, Liew A, Reiter L, Flatt RJ, Van Mele T, et al. Structural design, digital fabrication and construction of the cable-net and knitted formwork of the KnitCandela concrete shell. Structures 2021;31:1287–99.

[17] Popescu M. KnitCrete: Stay-in-place knitted formworks for complex concrete structures. ETH Zurich 2019. https://doi.org/10.3929/ETHZ-B-000408640.

[18] Bouten S, Popescu M, Ranaudo F, Van Mele T, Block P, Mengeot P, et al. Design of a funicular concrete bridge with knitted formwork. IABSE Congress Ghent 2021-structural engineering for future societal needs, Ghent, Belgium: 2021, p. 690–9. 10.2749/ghent.2021.0690.

[19] Lienhard J. Bending-active structures: Form-finding strategies using elastic deformation in static and kinematic systems and the structural potentials therein. Universität Stuttgart; 2014.

[20] Cuvilliers P, Douthe C, du Peloux L, Le Roy R. Hybrid structural skin: Prototype of a GFRP elastic gridshell braced by a fiber-reinforced concrete envelope. J Int Assoc Shell Spatial Struct 2017;58(1):65–78.

[21] Popescu M, Reiter L, Liew A, Van Mele T, Flatt R, Block P. Building in concrete with an ultra-lightweight knitted stay-in-place formwork: prototype of a concrete shell bridge. Structures 2018;14:322–32. https://doi.org/10.1016/j.istruc.2018.03.001.

[22] Winn JJB. Development of shell structures without formwork. New building research spring. In: Proceedings of a conference presented as part of the 1961 spring conferences of the Building Research Institute, Michigan. USA: National Academy of Science - National Research Council; 1961. p. 1961.

[23] Marsh III JH. Construction of thin shell structures by the "Lift-Shape" process. In: Proceedings of the World Conference on Shell Structures, vol. 1187, University of California, Berkeley: National Research Council, National Academy of Sciences; 1962, p. 447–52.

[24] Tang G, Pedreschi R. Deployable gridshells as formwork for concrete shells. In: Proceedings of the International Society of Flexible Formwork (ISOFF) Symposium 2015, Amsterdam, The Netherlands: 2015.

[25] Shah A, Irani S. Design and construction of a novel slab system using bending-active framework. In: Proceedings of the International fib Symposium on Conceptual Design of Structures, Madrid, Spain: 2019, p. 329–36.

[26] Harris R, Kelly O, Dickson M. Downland gridshell—an innovation in timber design. Proc Inst Civil Eng - Civil Eng 2003;156(1):26–33.

[27] SOFiSTiK AG. SOFiSTiK 2020.

[28] Bellmann J. Active bending starting on curved architectural shape. In: Bletzinger K–U, Oñate E, Kröplin B, editors. 8th International conference on textile composites and inflatable structures - structural membranes 2017, Munich, Germany; 2017.

[29] Magarò A, Baratta A. Palazzetto dello Sport. Architetture al cubo. 2016th ed., Rome, Italy: 2018, p. 96–113.

[30] Hauschild M, Karzel R. Digital processes: planning, design, production. Basel, Switzerland: Birkhäuser; 2011.

[31] Hack N, Dörfler K, Walzer AN, Wangler T, Mata-Falcón J, Kumar N, et al. Structural stay-in-place formwork for robotic in situ fabrication of non-standard concrete structures: A real scale architectural demonstrator. Autom Constr 2020;115:103197.

[32] Ciorra P, Casciato M. Technoscape. L'architettura dell'ingegneria | MAXXI 2022. https://www.maxxi.art/en/events/technoscape-larchitettura-dellingegneria/ (accessed November 28, 2022).

[33] Otto F, Bach K, Burkhardt B. IL 18: Seifenblasen. Stuttgart, Germany: Karl Krämer Verlag; 1988.

[34] Waimer F, Noack T, Schmid A, Bechmann R. From informed parametric design to fabrication: The complex reinforced concrete shell of the railway station Stuttgart 21. In: Gengnagel C, Baverel O, Burry J, Ramsgaard Thomsen M, Weinzierl S, editors. Impact: Design with all senses. Cham: Springer International Publishing; 2020. p. 390–400. https://doi.org/10.1007/978-3-030-29829-6_31.

[35] Scheder-Bieschin L, Spiekermann K, Popescu M, Bodea S, Van Mele T, Block P. Design-to-fabrication workflow for bending-active gridshells as stay-in-place falsework and reinforcement for ribbed concrete shell structures. In: Gengnagel C, Baverel O, Betti G, Popescu M, Thomsen MR, Wurm J, editors. Design modelling symposium - towards radical regeneration. Cham: Springer International Publishing; 2022. p. 501–15. https://doi.org/10.1007/978-3-031-13249-0_40.

[36] Rippmann M, Lachauer L, Block P. Interactive vault design. Int J Space Struct 2012; 27:219–30. https://doi.org/10.1260/0266-3511.27.4.219.

[37] Rombouts J, Liew A, Lombaert G, De Laet L, Block P, Schevenels M. Designing bending-active gridshells as falsework for concrete shells through numerical optimization. Eng Struct 2021;240:112352. https://doi.org/10.1016/j.engstruct.2021.112352.

[38] Liew A, Stürz YR, Guillaume S, Van Mele T, Smith RS, Block P. Active control of a rod-net formwork system prototype. Autom Constr 2018;96:128–40. https://doi.org/10.1016/j.autcon.2018.09.002.

[39] Aldinger L, Margariti G, Körner A, Suzuki S, Knippers J. Tailoring Self-Formation: Fabrication and simulation of membrane-actuated stiffness gradient composites. In: Mueller C, Adriaenssens S, editors. Proceedings of the IASS symposium 2018: creativity in structural design, Cambridge, USA: 2018.

[40] Lee M, Mata-Falcón J, Kaufmann W. Shear strength of concrete beams using stay-in-place flexible formworks with integrated transverse textile reinforcement. Eng Struct 2022;271:114970. https://doi.org/10.1016/j.engstruct.2022.114970.